Estimated Droop Control for Parallel Connected Voltage Source Inverters

Stability Enhancement

Beräkning av spänningsreglering för parallellkopplade nätomvandlare
Förbättring av stabilitet

Faisal Mahmood Ahmed

Faculty of Health, Science and Technology

Master's Program in Electrical Engineering

Degree Project of 15 credit points

Supervisors: Siriluk Pumirat. Fraunhofer IWES Kassel, Germany & Dr. Jorge Solis. Karlstad University, Sweden

Examiner: Arild Moldsvor. Karlstad University, Sweden

Date: 2013.12.30

Serial number

"Success is the result of foresight and resolution, foresight depends upon deep thinking and planning and the most important factor of planning is to keep your secrets to yourself."

Imam Ali(A.S.)

Abstract

Renewable Energy Sources (RES) are considered as the replacement of conventional energy sources. These RES can use wind energy, solar light, bio waste and can also be in the form of small hydro power units. These RES has very poor power quality and contains voltage fluctuations and variable frequency. These factors make RES a stability risk for the main utility grid. As a solution, currently inverters with different design techniques are being used as an interface between RES and main utility grid. The current study proposed a new technique "estimated droop control" for inverter design. The conventional droop control technique which was already used in inverter design, has difficulty in synchronizing parallel connected inverters with different droop gains and line impedances. The proposed "estimated droop control" does not use any predefined droop values for inverters and all inverters are responsible for the estimation of their own droop values with respect to their output power. Therefore, inverters are not bound to use same and static droop values which are considered as a vital communication link. The proposed design methodology has made inverters independent from this only virtual link of communication due to which the reliability of a system has increased. The proposed design technique has given very good results in a simulation run. When the Simulink model was run in parallel connected inverter with different line impedances, it was a success as both inverters started operating with same droop values as they were sharing an equal load. The most important test was with different line impedances because in conventional droop control it is difficult for inverters to keep their synchronism with different line impedances and an unequal load sharing make inverters to deviate from their nominal values and to generate different tracking signals for each set. This problem has been successfully solved with estimated droop control as in this method each inverter set its droop gains according to its output power, which helps an inverter to operate at nominal values with different droop gains and line impedance.

Acknowledgements

I would like to use this opportunity to express my gratitude to my advisor Mrs. Siriluk Pumirat, for her guidance and supervision throughout my work. She has always encouraged and motivated me to use my technical skills to achieve set goals.

Then I would like to thank Dr. Jorge Solis for his support and kind suggestions. I truly admire his dedication towards his profession and students. It is a great opportunity for me to work under his supervision.

In the end, I would like to express my deepest gratitude to *My Parents*, for their love and support since I have opened my eyes in this world. They have always given me a self possession and self reliance to excel and progress in life.

Contents

List of Figures

List of Tables

Abbreviations

RES	Renewable Energy Sources
DG	Distributed Generation
SCIG	squirrel cage induction generator
WRIG	wound rotor induction generator
DFIG	doubly fed induction generator
PV	Photo Voltaic
MG	Micro Grid
Sync-Gen	Synchronous Generator
AC	Alternating Current
DC	Direct Current
VSI	Voltage Source Inverter
PWM	Pulse Width Modulated
LV	Low Voltage
CPL	Constant Power Load
CIL	Constant Impedance Load
IGBT	Insulated Gate Bipolar Transistor
BJT	Bipolar Junction Transistor
SOGI	Second Order Generalized Integrator
PLL	Phase Locked Loop
RMS	Root Mean Square
PI	Proportional Integral
PR	Proportional Resonant
THD	Total Harmonic Distortion
GM	Gain Margin
PM	Phase Margin

Dedicated to My Parents does not matter how far they are living,
in fact they are always very close to my heart.

Chapter 1

Introduction

The global demand for energy is rising day by day and people are thinking about alternative solutions. Therefore renewable energy sources (RES) are getting more and more popular now a day. The motivation behind these efforts is to utilize the free energy which is already present in nature without affecting the environment and producing greenhouse gases. Many countries have decided to reduce 20% emission of greenhouse gases by the end of 2020 [1], Denmark has already achieved this goal by producing 20% of electricity through RES. In this regard Germany is planning to generate 100% Electric energy through RES until 2050. The conventional system of producing electricity through fossil fuel is causing environmental pollution which is resulting in global warming and very abrupt changes in weathers all over the world. Another reason is increasing in prices of fossil fuels which has increased the production cost of electricity and also fossil fuel reserves are limited. So these circumstances make nations think about unlimited and clean energy at minimum price.

1.1 Renewable Energy Sources

In the near future, changes in present transmission and distribution systems are expected to occur on a very large scale and may be the largest portion of electric power demand will be shifted to RES. These RES include wind energy, solar energy, biomass, fuel cells and small hydro units. These RES units can be installed near to the load centres to meet the load demand locally. These RES also known as Distributed Generation (DG) units [2]. Figure 1.1 shows most common RES used as distributed generation units.

These DG units can operate in autonomous mode which facilitates a commercial consumer in different ways like low cost for transmission systems, reactive power and harmonic compensation, power factor correction and backup generation which may not be

possible in a centralized system. These DG units can be easily plugged in or plugged out from the utility grid in case of failure without affecting the system[2].

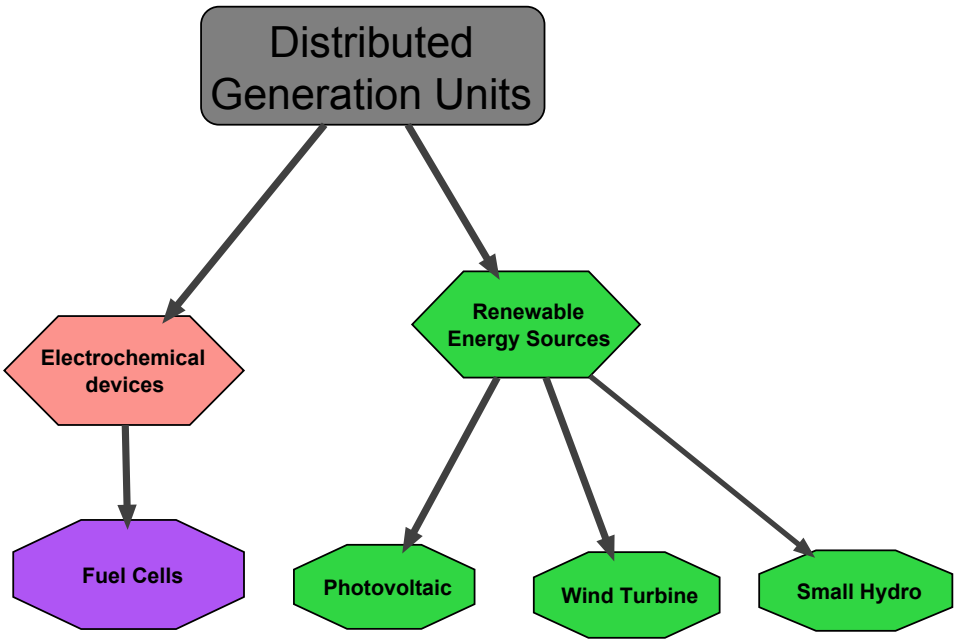

FIGURE 1.1: Different distributed generation units.

A number of small generation units which have a capacity less than 250kW are already in use for peak shaving and also as a back up generator. In the following sections their features have been discussed briefly. A brief analysis of different DG units is shown in Table 1.1.

1.1.1 Wind Energy

Wind Energy is transformed into electricity through a wind turbine which consists of large blades, generator, energy storage, gearbox and power converters. The efficiency of a wind turbine to produce electric power depends on blades and generator which is directly connected to the blades and rotates as wind rotates the blades of the turbine. Now a days large wind farms have been harvested to generate electrical energy which is also Eco friendly. The capacity of generated power mainly depends on the speed of wind, therefore wind farms are installed in best wind corridors to have maximum wind flow. The efficiency of electric energy produced by these wind farms is approximately from 20-40% and the capacity of a single wind turbine ranges from 0.3kW to 5MW [2–6].

The wind turbine has the following categories [3, 7]:

1. Fixed speed wind turbine which uses squirrel cage induction generator (SCIG).
2. Partial variable speed wind turbine uses a wound rotor induction generator (WRIG).
3. Variable speed wind turbine with partial frequency converter uses a doubly fed induction generator (DFIG).
4. Variable speed wind turbine with full power inverter and converter and uses either SCIG or WRIG.

1.1.2 Solar Energy

Solar energy is utilized through photo voltaic (PV) panel which is an array of interconnected cells made of doped silicon crystals, batteries and power converters. Power generation capacity of PV varies from 0.3kW to few MW. Recently, a large PV unit has been developed in the UAE with capacity of around 250MW [8, 9]. As power generation from PV depends on the intensity of sunlight therefore its efficiency to generate electric power is not uniform. PV panels over an acre of land can produce approximately 150kW [10]. Main problems in PV system are voltage fluctuation and weak harmonic injection. This problem can be solved with an internal control for a PV system, which gives good power tracking and processing [2]. Many research institutes are also working to improve the cell structure of PV systems, in order to increase the efficiency of a system. Power Inverter is needed to integrate a PV system to the main utility grid.

1.1.3 Fuel Cells

In fuel cell, chemical energy is used to produce electric power through an electrochemical process. It works as a battery to produce electric power but it needs a continuous supply of fuel which is generally in the form of natural gas, gasoline, bio gas or propane, while a battery needs a charging system. Capacity of fuel cell depends on sources in which it is being used that may be a portable or stationary source [2]. The fuel cell also needs a power inverter to interface with the main utility grid.

1.1.4 Micro Turbines

These turbines usually consist of small combustion engines that can be run with bio gas, natural gas and other types of fuel. These turbines have a capacity from 20-500kW.

TABLE 1.1: Comparison of different energy sources

	Micro Turbines	Wind Turbines	Photovoltaic	Fuel Cells	Fossil fuel Generator
Rating	20-500kW	1kW-5MW	0.3kW-2MW	1kW-5M	Few hundred MW
Capital Cost ($/kW)	900	3000	5500	2800	500-900
Efficiency	20-30%	20-40%	5-15%	40-60%	33%
Fuel	Natural-gas, Hydrogen, Bio-gas, Propane, Diesel	Wind	Sunlight	Hydrogen, Natural-gas, Propane	Furnace-oil, Diesel, Natural-gas, Coal, etc.
Grid/Load interfacing	Power Electronics	Power Electronics	Power Electronics	Power Electronics	Synchronous Generator

These turbines are faster in speed and evolves less temperatures. Their main advantage is the ease in their mobility from one place to another because of their small size. Secondly they are easy to install, low cost and need less maintenance. These turbines can be integrated to the main utility grid through inverters [11–14].

1.1.5 Other RES

Bio mass can be used to produce bio gas which is then fed to a gas turbine to produce electricity. Micro hydro units can be placed on small dams, on the edge of rivers, canals and springs where the flow of water is used to run a turbine to produce electricity.

1.2 Problems related to RES

The amount of power available from single RES is not enough to meet the demand and different RES produces power during different spans of time and may not be able to form a grid. This gives an idea of a Micro Grid (MG), an MG consists of two or more DG units. These DG units can be operated either by the same kind of energy sources or different like wind, solar and hydro sources. Therefore these units may have high frequency (high speed) units like hydro, low frequency (slow speed) like wind turbines or those sources which produce DC voltage or current like fuel cells or PV sources. Due to this random nature of RES it is not suitable to inject the output power of RES directly into the utility grid or for the direct utilization by consumers. This can also make the whole system unstable.

As RES mostly depends on natural factors like speed of wind and intensity of sunlight which is not in human control, therefore some kind of storage facility is required in case of no load or low load times. These storage units can also help to process the output power to make it suitable for main utility grid or domestic load. There is also another issue of synchronization among different DG units within an MG and between main the utility grid and MG.

1.3 Background and Motivation

There are different types of power generators in a microgrid and it is very important to keep control over all these generators. This control is responsible for equal power sharing and for regulating voltage amplitude and frequency. There are two types of control schemes:

1. Communication based control.
2. Non-communication based control.

In communication based control, a supervisory control over all generators is needed. This supervisory control receives information from all terminal generators and try to keep balance in power sharing among these generators. This technique is not very reliable as it needs high bandwidth communication link for fast sharing of information. This control is not feasible when generators in microgrid are spread over a vast area and there is a long distance between them. If this supervisory control or master control fails due to any reason then the whole system may stop working. In this case another problem of dispatching these generators in microgrid will be possible.

A non-communication based technique enables every unit in microgrid to regulate their output voltage and frequency so these units can share active and reactive power demand accordingly. This technique uses a method of frequency and voltage droops as in conventional power system generators [15]. This control allows every unit to change active and reactive load if there is any change happens in frequency or voltage of a system respectively [2]. These frequency and voltage droops act as a vital communication link.

A non-communication based control increases the reliability of a system as all units are independent and responsible for their individual control of frequency and voltage. This advantage gives a motivation to use droop control for DG units in microgrid. This technique is also not a perfect one, it still needs improvements. There are a few drawbacks in this technique i.e. due to droop characteristics, frequency and voltage of

DG units may drop to a lower level values different from the nominal values [2]. Secondly if the difference in voltage and frequency is beyond a certain range then it is difficult to synchronize DG units. This happens when the distance between DG units is large which results in different line impedances for every unit. This project work is carried out to address these two above mentioned problems so that every unit can regulate its voltage amplitude and frequency at or around specific set references. The main goal of this thesis work is to operate DG units in microgrid with almost same amplitude and frequency so that they can keep synchronization almost in every case.

1.4 Objectives of thesis

Problem Defination: *Output power of RES needs a proper processing through an inverter before utilizing by the consumer. Secondly the most important goal is the synchronization among parallel connected inverter. This synchronization is mostly affected when there are different line impedances among inverters and they have different droop gains. Another main concern is to achieve the stability of a system. The stability of a system is most affected by different kind of linear and non-linear load variations.* The following objectives have been tried to achieve from this thesis work:

- The very first objective is to achieve Voltage and frequency control. These two parameters are very essential for the synchronization of all DG units in an MG. Disturbances in the form of load variation directly affect the voltage and frequency.
- Load sharing among inverter based DG units is also a key phenomena. So, in this thesis work it has been tried that inverters share equal load, if there is a situation in which it is not possible to share the load equally then at least inverters should be capable to keep their synchronism.
- The third objective is to develop a non-communication based design for parallel connected inverters. This will help to reduce the cost of a system and also increase the reliability of a system. If these inverters have to share the information then their dependency on each other will increase which can affect the autonomous operation of each inverter. It is in vast favour to make each inverter as much independent in its operation as possible.

1.5 Overview

The rest of the thesis is structured as follows:

Chapter 2 will present a brief background of traditional electric power systems and modern state of the art inverter dominated MG.

Chapter 3 will discuss the different control strategies for inverters and give a brief comparison. This chapter will present a mathematical model of plant. This chapter will also discuss the droop control technique using estimation theory and discuss different tools which have been used to achieve set goals.

Chapter 4 will present the model analysis in frequency domain and time domain. This chapter will also discuss the simulation results for both traditional droop control and estimated droop control technique.

Chapter 5 will conclude all this thesis work and propose directions for future work.

Chapter 2

Power Generation and Power Network Technology

2.1 Conventional Power system structure

The stability of a power system means synchronization of two machines or two groups of machines. The stability of a system will lose if machines lose their synchronism but there is another case in which instability may even occur without losing synchronism because of disturbances.

First of all this chapter will discuss and analyse the effect of different kinds of disturbances acting on a system. Disturbance means the effect of random events on the system either intentionally or unintentionally. Disturbance can be modelled by changing parameters or by changing non-zero initial conditions of differential equations [16–18].

If a linear system is stable for small disturbances then it will also be stable for large disturbances. But if a nonlinear system is stable for small disturbances then such a system may or may not be stable for large disturbances. The large disturbance which can make a system unstable is called *critical disturbance* [16–18]. Stability mainly concerns about the response of a system towards:

1. Change in demand for power

   In case of any change in demand for power, the response of a system is very fast for transfer of energy from generator to load but slightly slow for voltage and frequency control and slow for adjustment of power generation [16–18].

2. Various types of disturbances

The response of a system under different kind of disturbances is fast for wave phenomena in transmission line due to electromagnetic changes in electrical machines and slowest for prime mover and automatic generation control actions to take effect [16–18].

Real power depends on the product of phase voltages and the $\sin(\delta)$. This δ is an angle between two phasor voltages known as *rotor angle* or *power angle*. Small variations or disturbances cannot influence the active or real power(P) [16–18].

While the reactive power (Q) depends on the difference in the magnitude of two phase voltages. Small variations in voltages can bring large changes in the system [16–18].

Stable system ensures good quality of the output power which means defined level of voltage with low fluctuations and also defined value of frequency with low fluctuations plus low harmonic contents [16–18].

2.1.1 Important parameters for stability

There are three very basic key parameters involved in deciding the stability of a system and these are briefly described as follows:

1. Rotor angle

   Rotor angle stability involves the study of electromagnetic oscillations in an electric power system. Every synchronous machine has electric torque and this electrical torque is further resolved in synchronous torque and damping torque. If the synchronous torque is reduced then there will be an aperiodic drift in rotor angle which leads a system towards instability. Similarly if the system does not have a sufficient damping torque this will result in an oscillatory behaviour of a system which will finally cause instability [17].

2. Voltage stability

   The ability of a system to maintain steady state voltage on all the buses in a power system under normal operating conditions and also after disturbances. Instability occurs because of increase in load and change in system conditions which leads to a progressive and uncontrollable drop in voltage. The inability of a system to meet the demand of reactive power and also due to the flow of active and reactive power simultaneously through the inductive reactances of the distribution system.

   If the reactive power is injected into one of the buses then it should increase the voltage of all buses not just on that specific bus. So that, the criteria is there

should be a collective increase or decrease in the output reactive power on all buses. This results in a balanced system [17].

2.1.2 Synchronous generator(Sync-Gen)

There are two categories of generators:

1. High speed generators

   Such generators are used in steam and coal turbines. This kind of generators has short *diameter* and large *axial length*. Typically have 2-poles (driven at 3000rpm) and 4-poles (driven at 1500rpm) [16]. In figure 2.1 (a) a speed generator with four poles can be seen which has long axial length and short diameter. Similarly in figure 2.1 (b) a high speed generator with two poles can be seen.

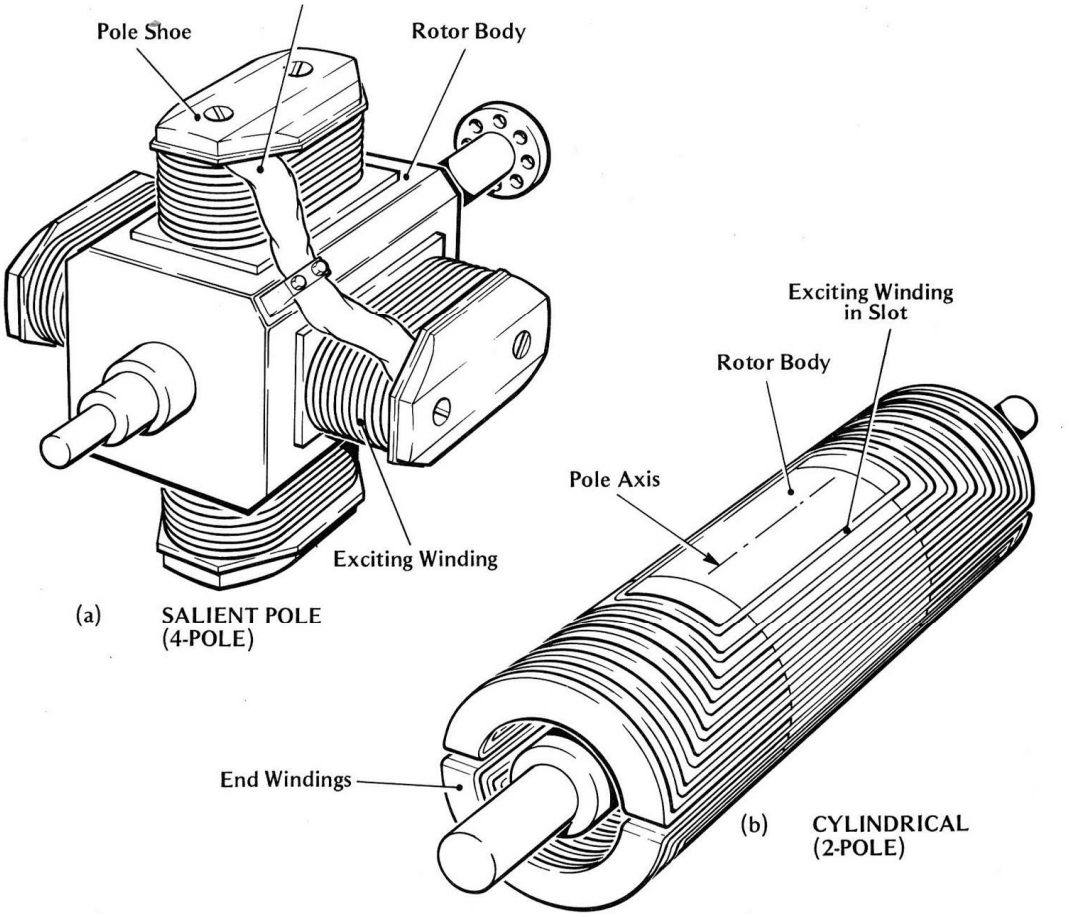

FIGURE 2.1: High speed 4-Pole and 2-Pole generator [19].

2. Low speed generators

Such generators have short *axial length* and they have a large number of poles and are normally driven at 500rpm or less [16]. A low speed generator with large number of poles is shown in figure 2.2.

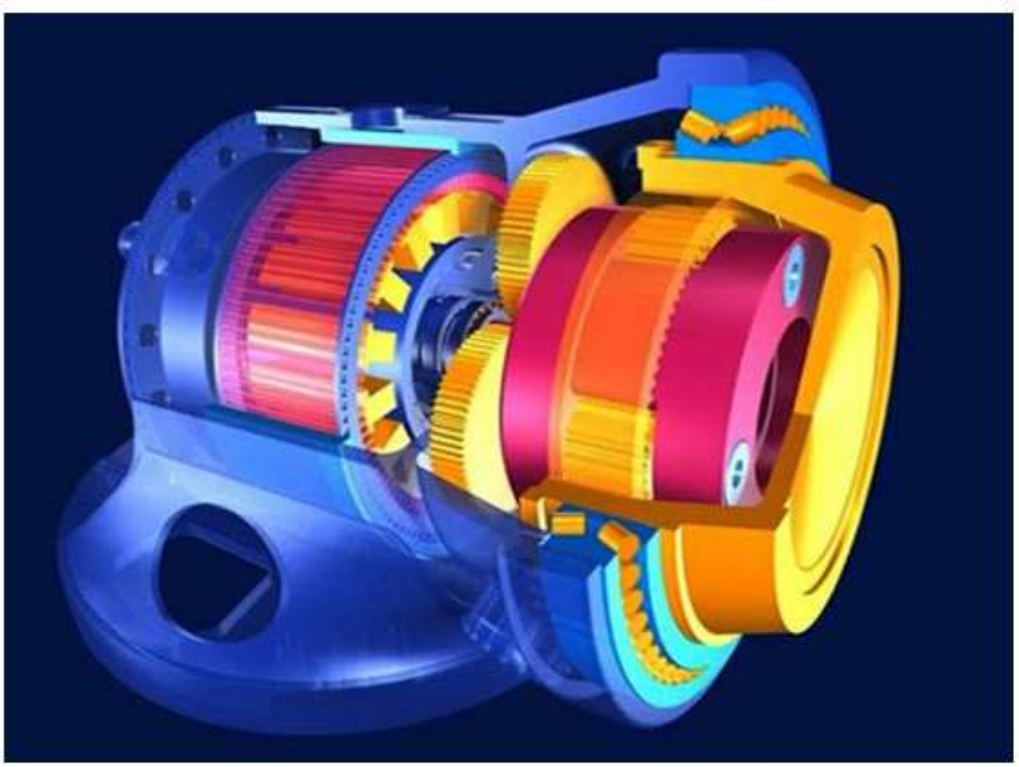

FIGURE 2.2: Low speed generator [20].

The number of magnetic poles depends on the required speed and the nominal frequency of the power system. A generator has two main magnetic parts *stator* and *rotor*. A prime mover rotates the *rotor* this produces a magnetic field and induces current in the 3-phase *stator* winding [16].

2.2 New Power system structure

2.2.1 Inverter

In previous sections, the term *Inverter* is being used extensively. In the integration of RES or to form an MG, an inverter is an essential part of the system. It comes under the category of power electronics, it performs DC to AC conversion and produces a sinusoidal output voltage. The frequency and magnitude of this sinusoidal output can be controlled. An inverter which has a DC voltage source as an input is called the voltage source inverter(VSI) [21, 22]. There are three categories of VSI:

1. Pulse width modulated inverter.
2. Square wave inverter.
3. Single phase inverter with voltage cancellation.

In this thesis work, pulse width modulated (PWM) single phase full bridge inverter is used as shown in figure 2.3. This PWM based inverter uses constant DC voltage source as input therefore magnitude of inverter output voltage and frequency needs to be controlled. This control is achieved through PWM signal for inverter switches to keep AC output voltage as much close to a sine wave as possible [21]. The main disadvantage of second scheme is that their output AC voltage waveform is more like a square wave than a sine wave. Single phase inverter with voltage cancellation can only be used as a single phase system, not as a three phase [21].

Basically an inverter is a combination of switches and PWM which generates a signal to turn these switches on and off. This PWM consists of a triangular wave generator (which is a carrier signal) and a sinusoidal signal (a control signal) which is then compared with triangular wave to have a modulated signal [21, 22]. This topic is discussed in detail in section 3.2 chapter 3.

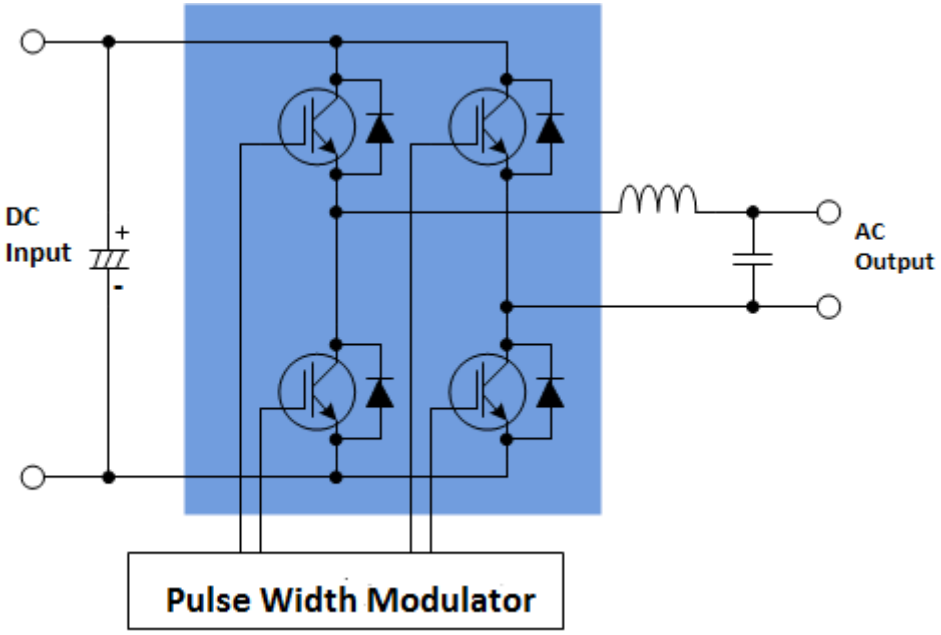

FIGURE 2.3: Single phase full bridge inverter

2.2.2 MicroGrids

DG units do not have stable output power which makes them unsuitable to connect with the main distribution system. Microgrid system is now emerging as a best solution to this problem which consists of multiple DG units to provide electrical power in the local domain. Microgrids minimize the Impact of DG units on the safety and performance of the main utility grid, which gives the possibility to shut down in case of any fault. Before microgrids, limited number of DG units can be connected to the utility grid but with microgrids it is easy to connect large numbers of DG units [23–25]. Microgrid system has small power scale but this system still faces some complexities like:

1. An inverter dominated micro grid is very sensitive towards disturbances because it does not have inertia like conventional power system generators. Load variations, the interaction of an inverter with other inverters or network and even power sharing error can act as severe disturbances for a MG [2].
2. A MG can easily get unstable because it has limited capability to handle overload situations which is a result of a circulating current. Similarly low damping in power sharing mechanism also plays its role to make MG unstable [2].
3. Another challenging task is to have a good power sharing mechanism among different units in MG. One solution is to use communication links between each unit so that they can share their information but this solution is not only costly but the reliability of the system is also compromised. Secondly in remote areas this kind of solutions are not practical due to large distances between different DG units. So, it is in favour to have non-communication based power sharing mechanism in MG [2].

Structure of a Microgrid

The structure of microgrid is shown in figure 2.4 and it is explained as follows:

1. Point of common coupling where all DG units are connected [23].
2. Ability to operate in both island and grid connected mode through switch [23].
3. Use of power electronics as an interface between DG units and microgrid [23].
4. Control of active and reactive power of each unit, this can be achieved through inverter [23].
5. Protection from reverse power flow [23].

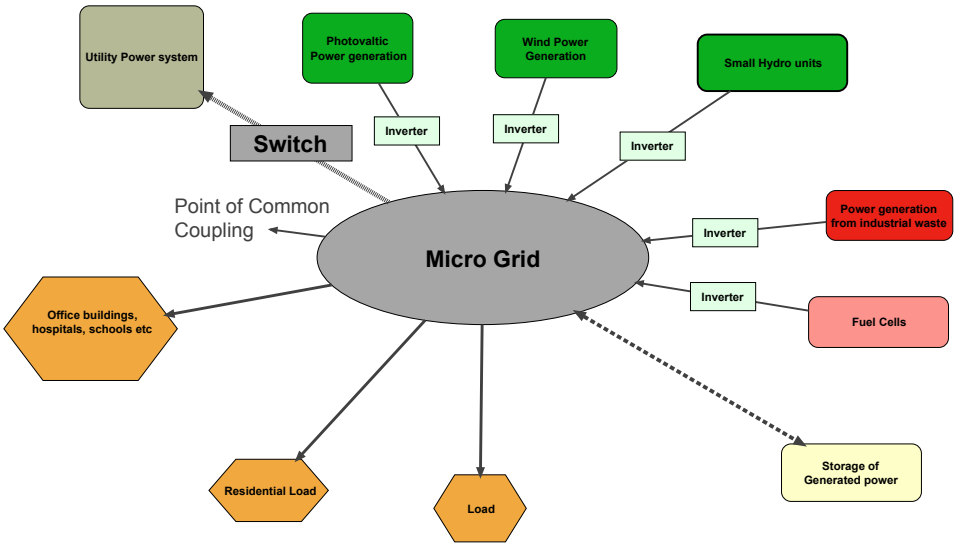

FIGURE 2.4: Micro Grid.

6. Energy storage unit in case of no load or low load [23].

Operation of a Microgrid

1. Microgrids can use droop control method to provide voltage and frequency support, when these two quantities deviate from their nominal values. In the past, tripping relays were in use to handle over voltage but now a days power curtailment method can be used to prevent the system from over voltage. This method can curtail the input voltage if the output voltage exceeds above a specific level and can also curtail load if the output power goes below a specific level. For maximum quality of service both voltage and frequency should operate in certain limit [23].

2. In low voltage (LV) island grids with resistive lines, the frequency of a power system can be controlled by regulating the reactive power. In virtual impedance method this can be achieved by controlling the phase angle of the AC voltage source relative to the grid voltage which is proportional to the rated and measured frequency. It is a storage unit that controls the frequency in suitable range using droop characteristics [23]. If frequency rises above the limit then by generating reactive power and if falls below the limit then by absorbing reactive power. Here

it is important to mention that if the system consists of inductive lines which is the most common case then the frequency is controlled by regulating active power.

3. Frequency and voltage tolerance or droops are used as a communication means in an MG. This technique does not require any communication links [23].

2.2.3 Constant power load(CPL)

Tightly regulated power electronics show negative impedance of their characteristics similar to constant power load. A system which is modelled in [24] shows that some of the poles lie on the right hand side in s-plan domain which shows that the system is not stable. Both voltage and current gains are tuned but the system remains unstable. Then the effect of constant power load and constant impedance load is studied in [24] and these parameters are tuned to stabilize the system which gives good results [24]. The following parameters can be tuned:

1. Higher $\frac{R}{L}$ ratio for feeder impedance linking load and DG units. Usually distributed level feeder have high $\frac{R}{L}$ ratio compare to the transmission line feeders [24].

2. By increasing the equivalent capacitor of two feeder lines by adding a filter capacitor [24].

3. By increasing operating voltage but this needs to change the whole configuration of microgrid system which is not feasible [24].

4. If CPL is connected in parallel with the constant inductive load (CIL), this will keep the system stable. For stable microgrid a suitable load should be connected while designing the system especially when microgrid have to operate in island mode [24].

2.2.4 Inverter dominated grid

Inverter dominated grids are inertia less. A stability algorithm cannot be designed unless the system has constant frequency. Grid forming units are responsible for regulating frequency and voltage to loads and P-Q controlled sources in isolation mode. P-Q controlled sources are used to support grid during faults in grid to keep the grid voltage at a constant level by injecting reactive power. These sources used to regulate reactive power and DC bus voltage which regulates active power. They are connected to the grid via voltage source inverter (VSI). Frequency and voltage are regulated via active and reactive power respectively similar to the droop curve characteristics of the conventional

generator source. In this case phase angle is calculated by integrating the frequency which is calculated by frequency droop curve [25].

A P-Q controlled source uses the internal AC voltage source (phase and magnitude) to keep the DC side voltage and reactive power at specified level. The difference between inverter output power and generated power of the primary source charges a capacitor whose first order differential equation gives DC voltage. The angle difference between the internal voltage of the inverter and the terminal voltage is equivalent to the power angle or the rotor angle of the Synch-Gen. It is derived from error in DC voltage by using PI controller [25].

As microgrid is disconnected from utility grid then DG units of the microgrid starts producing active and reactive power to the load immediately with a fall in frequency. As the load increases P and Q will also increase with a fall in frequency. If another DG unit is added into the system this will share the P and Q of the system so the value of P and Q will fall and frequency will rise [25].

2.2.5 Synchronization

According to the synchronization criteria phase angle, frequency and amplitude must be alike and if it is three phase then the voltage sequence of each phase should also be considered [26].

1. If there is a difference in the magnitude of two voltages across the circuit breaker this will produce a transient curve which will result in a huge voltage to ampere ratio (VAR) flow [26].

2. If there is a difference in frequencies and the circuit breaker is closed, then this difference in frequencies will cause a sudden active power flow until system achieves common frequency. So for stable operation, frequency difference should be between 0 to 0.1Hz [26].

3. Phase angle difference will cause a huge flow of active power when the switch is closed. Difference in zero crossing of two voltages is called phase angle difference [26].

   Synchronization of two power sources with different voltage sequence in 3-phase is just like the synchronization of two motors rotating in opposite direction [26].

Chapter 3

System Modeling and Design

3.1 Control Techniques for parallel connected inverters

Inverters are being used as an interface between main utility grid and RES. Inverters are responsible to process the output power with controllable voltage amplitude and frequency. This processed output power from different RES is then fed into a microgrid which are either operating in synchronized mode with main utility grid or in island mode.

This can be achieved when inverters are connected in parallel to one another as shown in figure 3.1, with tracking of the sinusoidal voltage signal. This parallel operation of inverters gives redundancy, reliability and the possibility to upgrade the whole system without any reconfiguration. This needs a very strong control over the amplitude and frequency of an output voltage to regulate very strictly and to limit the circulating current among inverters in microgrid. From last two decades, technology to operate inverters in parallel is widely being used by researchers. Different control techniques have been developed to attain the best possible results. These techniques are discussed briefly in the following sections.

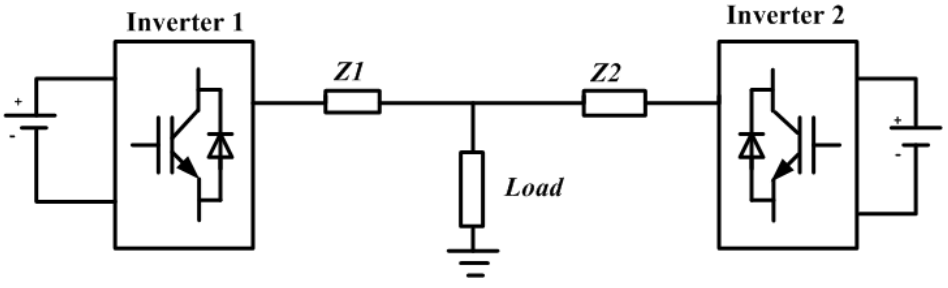

FIGURE 3.1: Two parallel connected inverters.

3.1.1 Master Slave control

In this control technique, one inverter act as a master while the rest of the inverters in the system are slaves to this main inverter. Master inverter operates in voltage controlled mode to control the output voltage of other slave inverters which operate in a current controlled mode. This method uses current controlled inverters in parallel with one voltage source inverter (master). This technique is useful when large numbers of inverters are connected in parallel.

The main disadvantages of this scheme are less reliability and redundancy. Whole system depends on master inverter if due to any fault in a system this master inverter stops its operation then the whole system will collapse. Secondly this method needs high bandwidth communication link to share information between master and slaves which increases the cost of a system. Many solutions have been proposed to address these issues like a random selection of a master, automatic selection of a new master on the failure of previous master and to choose an inverter as master with maximum power rating [27–29].

3.1.2 Instantaneous current sharing control

In this centralized control technique all inverters share information about the current shared among them. There are different categories to drive references for current like average current sharing, maximum current sharing and rotating reference current sharing [29]. This control system is considered as multiple input multiple output (MIMO) system as it gives and receives information from more than one inverter. There are several schemes to meet the requirement of accurate current sharing. One of them is to equally divide the load among all inverters in a system to detect an unbalanced current. It needs to regulate voltage and frequency to minimize active and reactive components of this detected current [30].

3.1.3 Voltage and Frequency droop control

This control technique is a non-communication based scheme which requires no communication links among inverters in a microgrid. This technique requires very less computational facilities and a simple microcontroller can be used to perform the task. Due to these advantages droop control not only increases the reliability of a system but also significantly reduces the cost of a system. The idea of a droop control in inverter dominated grid comes from the conventional Synch-Gen power system. In a conventional power system active and reactive power is controlled by regulating the angle difference

between the voltage phases of two AC machines and magnitude difference between two voltages respectively [29]. The same principle is followed in this technique to control the flow of active and reactive power by controlling the frequency and amplitude of the output voltage as shown in figure 3.2. When the flow of active power increases due to the increase in load, frequency of an inverter drops, similarly when the flow of reactive power increases then voltage will drop, this phenomena has explained in [25]. A certain acceptable range has defined for frequency and voltage droops which is 1% and 4% respectively from their reference values [31]. Adequate operating range is necessary for the sake of maximum quality of service [23]. Droop gains are represented by the slope of the line in figure 3.2. The fundamental droop equations for an inverter is given by

$$\omega = \omega_0 + m(P_0 - P) \tag{3.1}$$

$$E = E_0 + n(Q_0 - Q) \tag{3.2}$$

Where ω_0, E_0, P_0 and Q_0 are reference or rated values.

There are a few drawbacks in this control technique due to its droop characteristics. It might be possible that all inverter units in a system start operate with a new lower value for frequency and amplitude of system output voltage which are different from set point references. Secondly the lack of robustness can result in measurement error of voltage and current. This will further affect the measurement of a feedback signal (tracking signal) finally the power sharing mechanism will be disturbed [2].

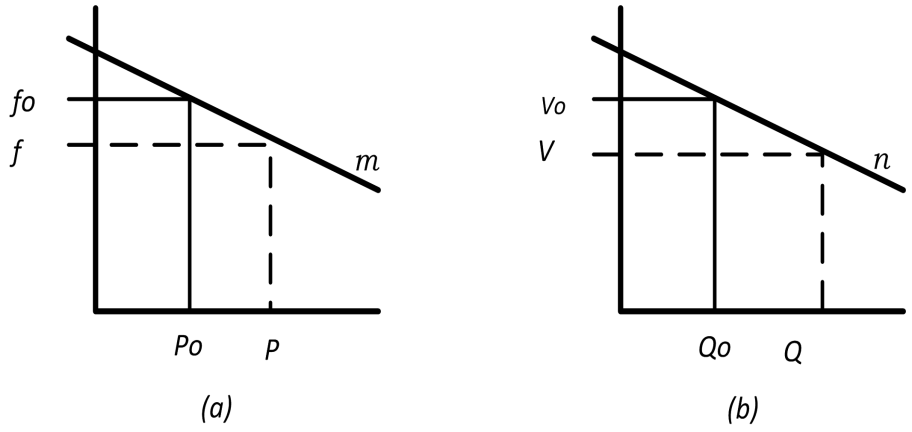

FIGURE 3.2: (a) Frquency and (b) Voltage droop curves.

This thesis work focuses on droop control technique because of its reliability, independence in the operation of every inverter unit and low cost makes it the best choice for microgrid. It might be a possibility that this technique will be considered as a standard scheme in the future for microgrids.

Many researchers are working to improve the performance of droop control scheme. In [32], a droop control technique is proposed in which high droop gains are used. High droop gains can give a better reactive power sharing among inverters in microgrid but simultaneously affect the stability of a system. A reactive power injection loop is used with the conventional droop control. This method does not require any communication link as it uses local measurements. There is an other method in [33] which gives better functioning of power-frequency droop by using arctan function. This method not only increases system stability but also gives natural frequency bounding between the two inverter system. There are many adaptive techniques have been proposed by Joseph M. Guerrero, who is trying to build a foundation to use advanced control techniques to improve the performance of a conventional droop control. In paper [34], an adaptive control method is proposed in which estimated voltage magnitude and frequency and the angle of grid impedance is used. This enables an inverter to independently inject active and reactive power into the grid. When two inverters are connected in parallel then there is a flow of circulating current between them during their transient period. This circulating current emerges due to initial voltage differences between two inverters. A solution to this problem is proposed in [35] which is to improve the response speed of controller during the transient state. If the duration of transient period is longer, then circulating current can damage an inverter. A virtual impedance method is proposed in [36] to have better reactive power sharing between parallel connected inverters regardless of the difference in line impedances and unequal sharing of non-linear load.

3.2 Inverter Design

Let's start with the introduction of very basic power semiconductor devices used in power electronic systems. There are four main groups of these semiconductors that are shown in figure 3.3.

1. Power diodes.
2. Thyristors.
3. Bipolar junction transistors(power).
4. Insulated gate bipolar transistors(IGBTs).

In inverters BJTs, IGBTs and MOSFETs are used and rated up to 1200V and 400A. BJTs can operate with 10kHz frequency and MOSFETs can operate even with higher frequencies up to several tens of kHz. MOSFETs usually have a limited rating like

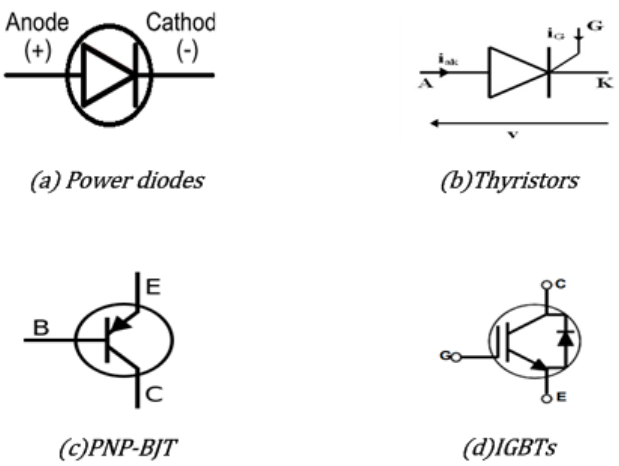

FIGURE 3.3: (a)Power diodes, (b)Thyristors, (c)PNP-BJTs, (d)IGBT [37]

1000V and 50A. Most IGBTs are being used in inverters because IGBTs is faster than BJTs and have better ratings than MOSFETs [37].

Let's define some terms first before proceeding with the discussion on the inverter. Amplitude and frequency of triangular wave (carrier signal) as V_{Tri} and f_{Tri} respectively. Then amplitude and frequency of sinusoidal wave (control signal) as V_{cnt} and f_{cnt} respectively. In the operation of an inverter, amplitude modulation (m_a) and frequency modulation (m_f) are very important for the signal generated by PWM generator. Because this very signal is responsible for the switching of IGBTs and switching speed is determined by the frequency of triangular wave f_{Tri}. These two signals (triangular and control) are compared as shown in figure 3.4 (a) to have a modulated signal for switching of IGBTs as shown in figure 3.4 (b). As much efficiently this switching is done, as much waveform of the output AC voltage will be close to a sine wave [21, 22]. The output of an inverter also contains harmonics at the frequency of triangular wave. The output signal of an inverter has a frequency equal to the frequency of a control signal f_{cnt}.

$$m_a = \frac{V_{cnt}}{V_{tri}} \tag{3.3}$$

It is a preference to keep m_a between 0 to 1. In this range the amplitude of a fundamental frequency component of the output voltage varies linearly, therefore this range is also known as linear range. All the harmonics are pushed around the switching or carrier frequency by PWM, while its multiples operate in the linear range. If there is an overmodulation means m_a goes beyond 1 then there will be many harmonics in output voltage as compare to linear range. Another drawback is that the amplitude of a fundamental frequency component of an output voltage will no more vary linearly [21].

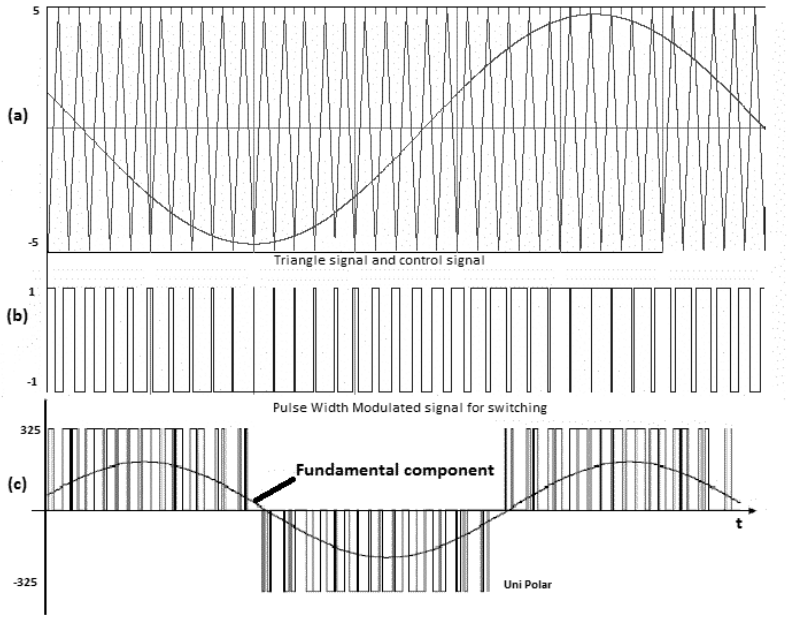

FIGURE 3.4: (a)Triangular and control signal, (b)Pulse width modulation, (c)Uni polar output of inverter

Switching frequency and frequency modulation index is also equally important as an amplitude modulation index in PWM. If switching frequency is higher then its easier to filter out undesired harmonics. Therefore it is suggested in [21] that either switching frequency should be less than 6kHz or higher than 20kHz. If there is a situation in which switching frequency has to be between 6kHz-20kHz, then let it be [21]. Because disadvantages of taking switching frequency above 20kHz will be more than the advantages. Frequency modulation index m_f sets the relationship between triangular wave (switching frequency = carrier frequency) and the control signal frequency [21].

$$m_f = \frac{f_{tri}}{f_{cnt}} \tag{3.4}$$

Due to m_f, PWM is placed in two types such as synchronous and asynchronous PWM. In synchronous PWM, both triangular wave and control signal wave are synchronized. For this synchronization m_f must be an integer, in case of single phase inverter, it should be an odd integer [21]. In asynchronous PWM there are subharmonics in the output voltage wave but small in amplitude for large values of m_f say above 100. This keeps the switching frequency constant while control signal frequency may keep varying as long as m_f is high [21].

It is important to note that the output of an inverter (just switches and PWM) is more like a square wave as shown in figure 3.4 (c). Therefore to have desired sine wave output

a filter is required with an inverter to filter out all unwanted harmonics.

3.3 Proposed Design

Before proceeding with system design it will be good to give an overview about what kind of design this thesis work is supposed to present. In section 3.1.3 droop control technique has been discussed with all its advantages and disadvantages. Some of the developments and improvements that have been made by different researcher are also described. Block diagram of the proposed droop control scheme is shown in figure 3.5.

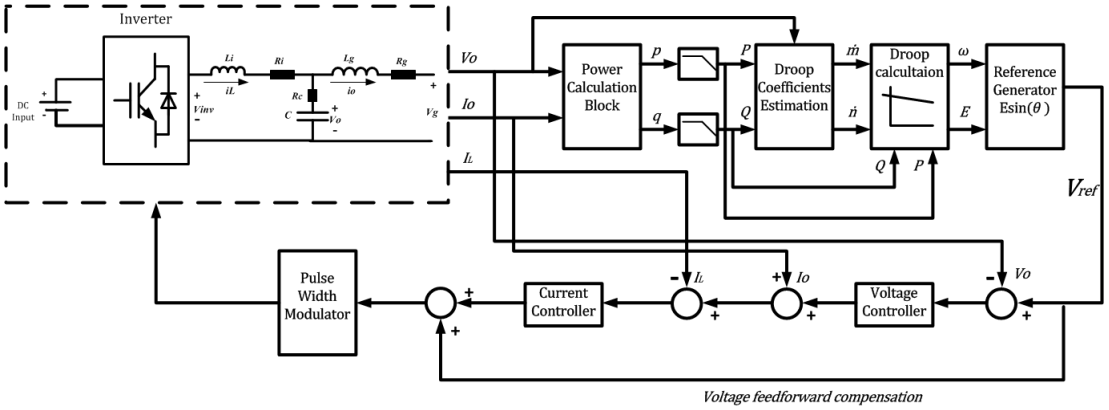

FIGURE 3.5: Single Phase Voltage Source Inverter

If this block diagram is compared to the block diagram of traditional droop control based inverters in [38, 39] or in some other articles, then the only prominent difference will be the droop coefficients estimation block. The traditional droop control scheme uses only fixed droop values for their droop control mechanism regardless of any change in output active and reactive power demand. While this thesis work has proposed a new droop control technique and this new estimated droop control block uses an online estimation mechanism for droop values rather than using fixed values (conventional method) and then these values are adapted by droop control block to control active and reactive power flow. Advantages and disadvantages of this technique will be discussed in next sections and chapter, when tests will be performed in Matlab/Simulink. The following tools have been used to assist this estimation process:

1. Second Order Generalized Integrator (SOGI)
2. Phase Locked Loop (PLL)

3.3.1 Second Order Generalized Integrator

In three phase system orthogonal components can be generated using either Clarke's transformation ($\alpha\beta$-components) or Park's transformation (dq-components) for stationary reference frame and synchronous reference frame respectively. Both transformations are shown below:

Clarke Transformation

$$\begin{bmatrix} u_\alpha \\ u_\beta \end{bmatrix} = \begin{bmatrix} \frac{2}{3} & \frac{-1}{3} & \frac{-1}{3} \\ 0 & \frac{1}{\sqrt{3}} & \frac{1}{\sqrt{3}} \end{bmatrix} \begin{bmatrix} u_a \\ u_b \\ u_c \end{bmatrix} \tag{3.5}$$

Park Transformation

$$\begin{bmatrix} u_d \\ u_q \end{bmatrix} = \begin{bmatrix} \cos(\omega t) & \cos(\omega t - \frac{2\pi}{3}) & \cos(\omega t + \frac{2\pi}{3}) \\ -\sin(\omega t) & -\sin(\omega t - \frac{2\pi}{3}) & -\sin(\omega t + \frac{2\pi}{3}) \end{bmatrix} \begin{bmatrix} u_a \\ u_b \\ u_c \end{bmatrix} \tag{3.6}$$

In a single phase system no space vector exists to help in the generation of orthogonal components. Therefore in single phase system, these transformation methods cannot be used to calculate amplitude, active and reactive power. A traditional method to calculate these parameters is to use a low pass filter and peak value detector [23]. Use of these algorithms requires a tradeoff between response speed to achieve steady state and undesired oscillations [23]. There is another way in which a delay function is used, in this method same signal is fed into the system twice first as it is without any modification which reflects as an in phase signal, α component and the second through a delay function to reflect β component as suggested in [40]. In this method the delay time has to be calculated very precisely and initial values will be zero for the signal through a delay block. To get rid of this trade off and delay calculation a second order band-pass filter with infinite gain at resonant frequency ω is used with low pass filter through a feedback.

$$G_{BP}(s) = \frac{Ks}{S^2 + \omega^2} \tag{3.7}$$

Above structure in Eq. (3.7) is known as "generalized integrator". This second order generalized integrator is being widely used in single phase system as it has been discussed in [31, 38, 39]. Therefore this thesis work is also using second order generalized

integrator technique for generating orthogonal components instead of the traditional method because of its better performance. The block diagram is shown in figure 3.6.

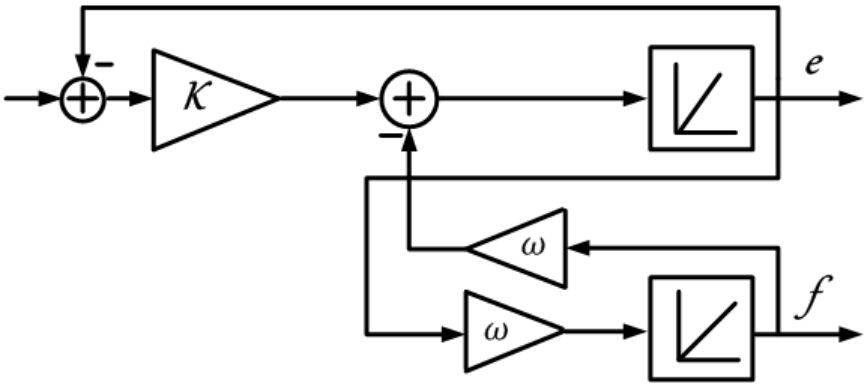

FIGURE 3.6: Second order generalized integrator

It can be seen from figure 3.6 second order generalized integrator has two outputs e and f. The e component is in phase with the input signal and f component has 90^0 phase shift and is lagging with respect to input signal. These two components have the same property as $\alpha\beta$ components in Clarke's transformation [23]. This structure can be used to generate orthogonal components for voltage and current, enabling better calculation of active and reactive power [23, 31]. Transfer functions for e and f are as follows:

$$G_e(s) = \frac{Ks}{s^2 + Ks + \omega^2} \tag{3.8}$$

$$G_f(s) = \frac{K\omega}{s^2 + Ks + \omega^2} \tag{3.9}$$

Where k is the gain and ω is the fundamental frequency

For single phase inverter, a second order generalized integrator is a best choice for the estimation or generation of orthogonal components. In figure 3.6, block diagram of basic second order generalized integrator (SOGI) has shown. The output of SOGI is shown in figure 3.7 and also compared to the input signal and step response. The orthogonal signals e and f are shown by green and red signal respectively. A dotted blue line is a step response of the system and the input signal is represented by black wave. The frequency of both input and output signals is same 50Hz. The response time of a system depends on the value of gain k [23].

If the value of gain k is higher then the response of a system will also be fast. There is also a limitation for gain k it cannot be very high because after a certain value there will be a start up overshoot which will not give a good estimation for orthogonal signals. This problem can also affect or damage the system. Reason behind this overshoot is

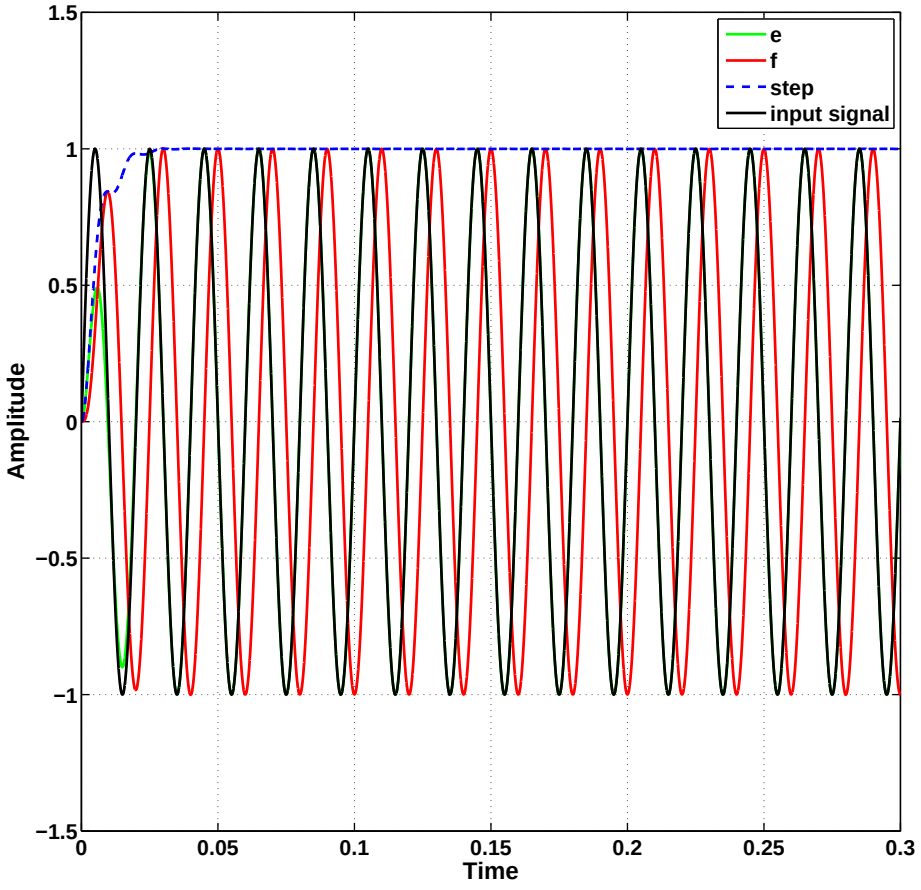

FIGURE 3.7: Operation of Second order generalized integrator

that the error signal can only correct the signal e and signal f is adjusted indirectly [23]. This phenomena can be seen in figure 3.8.

Kalman Estimation:

A new method based on Kalman estimation has been used by K. De Brabandere in [23] to improve the performance of SOGI. In this method, output signal f is also corrected directly by using a direct link to error signal through an extra gain k_2 like output signal e through a gain k_1. The block diagram is shown in figure 3.9 and transfer functions are given by

$$G_\alpha(s) = \frac{k_1 s - k_2 \omega}{s^2 + k_1 s + \omega^2 - k_2 \omega} \tag{3.10}$$

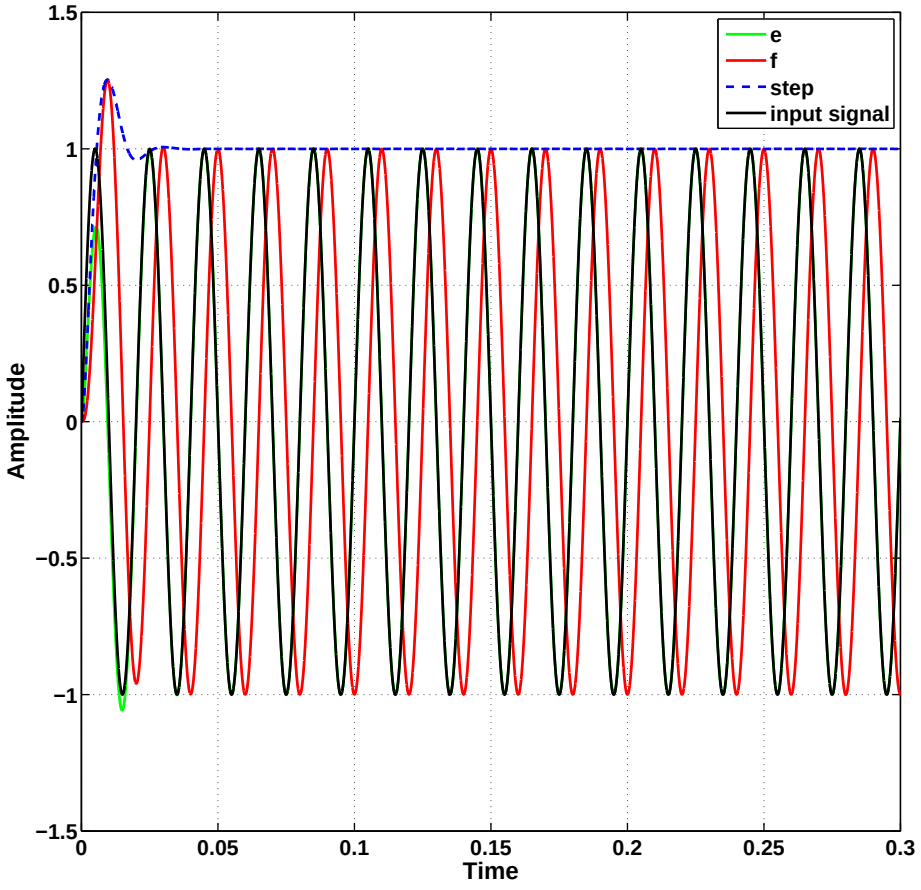

FIGURE 3.8: Operation of Second order generalized integrator with high gain k

$$G_\beta(s) = \frac{k_2 s + k_1 \omega}{s^2 + k_1 s + \omega^2 - k_2 \omega} \tag{3.11}$$

Where ω is the fundamental frequency.

There are different observer based estimation techniques that are in use and the choice of these techniques depend on either a given system is linear or nonlinear. Since the given SOGI is a linear system so, two methods have been proposed by Bjorn Sohlberg in [41] for linear system observers one is pole placement design and the second is Kalman filter. Pole placement design can only be used with single input single output (SISO) systems and the main drawback of this method is that it is a time invariant. While Kalman filter can be used for multiple input multiple output (MIMO) systems and the most important feature is Kalman filter can also be made time varying [41].

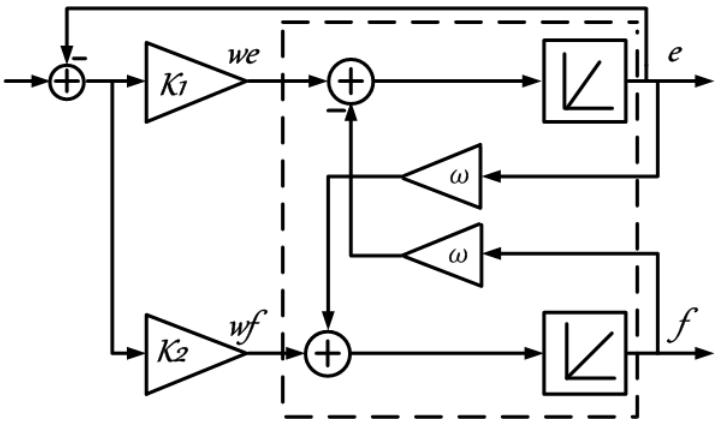

FIGURE 3.9: Second order generalized integrator with Kalman gain

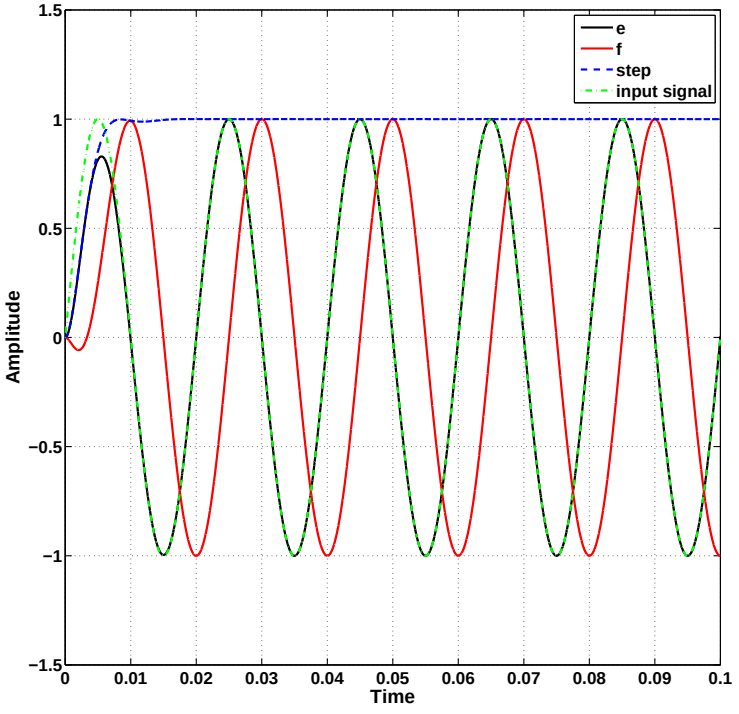

FIGURE 3.10: Second order generalized integrator with Kalman gains

A Kalman filter is an optimal estimator which means it can produce parameter of interest even from uncertain observations. Kalman filter can minimize mean square error of estimated states. Following features made Kalman filter a best choice for estimation in linear system [42]

1. Optimal approach of Kalman filter mostly ensures good results.

2. Give good results in real time online estimation which is needed for this thesis work.

3. Measurement equations need not to be inverted as this reduces the calculation and processing time.

In figure 3.9 an oscillator model is shown in dotted lines. This system has no measured input $u(t)$ to an oscillator except two white noise signals $w_e(t)$ and $w_f(t)$, there is only one measured output e. State space model of the system will be as follows:

$$\hat{x}(t) = Ax(t) + Bu(t) + Gw(t) \tag{3.12}$$

$$y(t) = Cx(t) + Du(t) + v(t) \tag{3.13}$$

where

$$A = \begin{bmatrix} 0 & -\omega \\ \omega & 0 \end{bmatrix}, G = \begin{bmatrix} 1 & 0 \\ 0 & 1 \end{bmatrix}, C = \begin{bmatrix} 1 & 0 \end{bmatrix} \tag{3.14}$$

$B = 0$ and $D = 0$ because there is not measure input u(t).

The Kalman state estimator is used for the calculation of SOGI gains k_1 and k_2. The Advantages of using Kalman estimator are that it gives optimal gain values and automatically places the poles at optimal locations while under the effect of white Gaussian noise and measurement noise. A detailed mathematical modelling and Matlab code for computer aided design is presented in **Appendix A**.

A Matlab function **kalman.m** is used for the calculation of Kalman gains. A sinusoidal signal (in this case output voltage signal V_0) is used as an input signal. At the output this block estimates two orthogonal signals with respect to one another. Output signal e will be in phase with the input signal and signal f will be lagging 90^o as described above.

Figure 3.10 shows the simulation result of the suggested scheme for SOGI with Kalman gains. It can be seen that the system reaches its maximum value very quickly and the response time is very fast without any overshoot. If higher values of Kalman gains are used, then this will not lead to a worse performance. This improvement is just because of k_2 because this is the only difference between two SOGI estimators.

3.3.2 Phase Locked Loop

Estimated orthogonal components can be further used with phase locked loop (PLL) for the estimation of system frequency as shown in figure 3.11. Design of a PLL discusses in detail in [43, 44]. A well designed PLL should have a narrow bandwidth for better noise rejection. Functioning of PLL depends on the performance of a PI block inside the PLL. A PLL will fail to lock at the desired frequency if the input signal has harmonics. If the difference between PI output and the desired frequency is more than the lock range or if the initial output of the PI is closer to harmonic components then PLL will fail to lock at the desired frequency. In grid connected mode the frequency of interest is 50Hz, to have a constant frequency PI controller in PLL should be tuned properly.

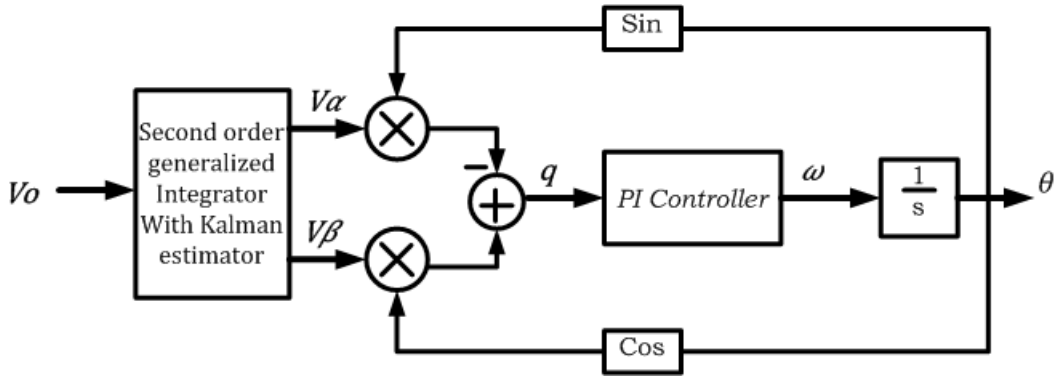

FIGURE 3.11: Phase Locked Loop

3.4 Plant Modelling

Inverter output voltage has harmonics due to high switching frequency around the fundamental frequency component of the output. It is necessary to filter out these high frequency harmonic components before connecting an inverter to load or in parallel to another inverter. A complete plant model is a combination of inverter and suitable output filter. There are three main types of filters are being used for inverter design [45].

- L Filter
- LC Filter
- LCL Filter

The choice of a filter depends on the application of the device. This thesis work has used an LCL filter as shown in figure 3.12 in order meet the requirement of lab apparatus.

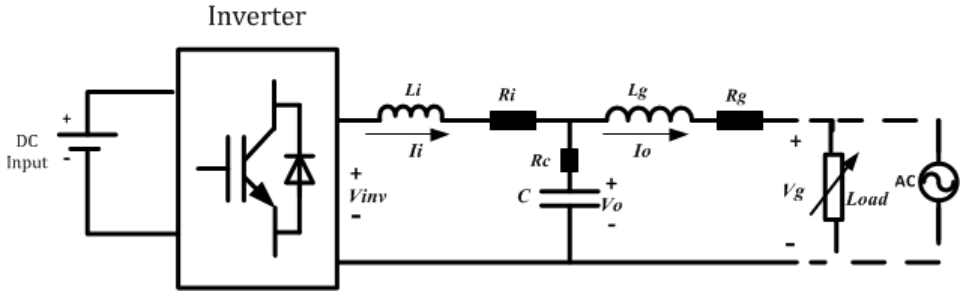

FIGURE 3.12: Inverter with LCL filter

An LCL filter provides better decoupling between the filter and grid impedance and also reduces the filter dependency on grid parameters. An LCL filter also attenuates frequencies above the resonant frequency by $60dB/decade$ [45, 46].

Following notation will be used for different system parameters:

- V_{inv} inverter voltage
- V_0 output voltage across filter capacitor
- V_g grid voltage
- I_i inverter current
- I_0 output current
- L_i inverter side inductance
- L_g grid side inductance
- C filter's capacitor
- R_i parasitic resistance of inverter side inductance
- R_g parasitic resistance of grid side inductance
- R_c filter capacitor's parasitic resistance

Let's apply Kirchoff's current and voltage laws to LCL filter shown in figure 3.5:

$$I_i - I_c - I_0 = 0 \tag{3.15}$$

$$V_{inv} - V_0 - V_i = 0 \tag{3.16}$$

$$V_i = L_i \frac{dI_i}{dt} + I_i R_i \tag{3.17}$$

By using Eq. (3.17) into Eq.(3.16) and rearranging

$$\frac{dI_i}{dt} = \frac{V_{inv}}{L_i} - \frac{V_0}{L_i} - \frac{I_i R_i}{L_i} \tag{3.18}$$

$$V_0 = \frac{1}{C}\int_0^t I_i(t) - I_0(t)dt \tag{3.19}$$

By taking derivative of Eq. 3.19

$$\frac{dV_0}{dt} = \frac{1}{C}(I_i - I_0) \tag{3.20}$$

$$\frac{dI_0}{dt} = \frac{V_0}{L_g} - \frac{V_g}{L_g} - \frac{I_0 R_g}{L_g} \tag{3.21}$$

For a state space model, let's suppose *X(t)* is a state vector which consists of state variables x_1,x_2 and x_3. A will be a state matrix, B_1 will be an input matrix, C will be an output matrix and B_2 will be a disturbance matrix. On the other hand *Y(t)* consists of output signals, *u(t)* has input signal and $u_g(t)$ has disturbance signals.

$$X(t) = Ax(t) + B_1 u(t) + B_2 u_g(t) \tag{3.22}$$

$$\begin{bmatrix} \dot{x_1} \\ \dot{x_2} \\ \dot{x_3} \end{bmatrix} = \begin{bmatrix} 0 & \frac{1}{C} & \frac{-1}{C} \\ \frac{-1}{L_i} & \frac{-R_i}{L_i} & 0 \\ \frac{1}{L_g} & 0 & \frac{R_g}{L_g} \end{bmatrix} \begin{bmatrix} x_1 \\ x_2 \\ x_3 \end{bmatrix} + \begin{bmatrix} 0 \\ \frac{1}{L_i} \\ 0 \end{bmatrix} \Big[B_1\Big] + \begin{bmatrix} 0 \\ 0 \\ \frac{-1}{L_g} \end{bmatrix} \Big[B_2\Big] \tag{3.23}$$

Where $\dot{x_1} = \dot{V_0}$, $\dot{x_2} = \dot{I_l}$ and $\dot{x_3} = \dot{I_0}$, $B_1 = u(t)$ and $B_2 = u_g(t)$. After putting these terms in Eq. 3.23 will result as follows:

$$\begin{bmatrix} \dot{V_0} \\ \dot{I_l} \\ \dot{I_0} \end{bmatrix} = \begin{bmatrix} 0 & \frac{1}{C} & \frac{-1}{C} \\ \frac{-1}{L_i} & \frac{-R_i}{L_i} & 0 \\ \frac{1}{L_g} & 0 & \frac{R_g}{L_g} \end{bmatrix} \begin{bmatrix} V_0 \\ I_l \\ I_0 \end{bmatrix} + \begin{bmatrix} 0 \\ \frac{1}{L_i} \\ 0 \end{bmatrix} \Big[u(t)\Big] + \begin{bmatrix} 0 \\ 0 \\ \frac{-1}{L_g} \end{bmatrix} \Big[u_g(t)\Big] \tag{3.24}$$

$$Y(t) = Cx(t) \tag{3.25}$$

$$\begin{bmatrix} y_1 = V_0 \\ y_2 = I_l \\ y_3 = I_0 \end{bmatrix} = \begin{bmatrix} 1 & 0 & 0 \\ 0 & 1 & 0 \\ 0 & 0 & 1 \end{bmatrix} \begin{bmatrix} V_0 \\ I_l \\ I_0 \end{bmatrix} \tag{3.26}$$

Now to have a transfer function model take the Laplace transform of Eq. (3.18), (3.19) and (3.21).

$$(sL_i + R_i)I_i = V_{inv} - V_0 \tag{3.27}$$

$$\left(\frac{1}{sC} + R_c\right) I_c = V_0 \tag{3.28}$$

$$(sL_g + R_g)I_0 = V_0 - V_g \tag{3.29}$$

Before proceeding further with the computation of filter transfer functions, there is a need for some assumption for mathematical analysis of a system. Lets suppose grid voltage is provided by an ideal voltage source and this ideal source of voltage is disconnected from inverter dominated MG, which will result in V_g=0 [45]. This assumption $V_g = 0$ means the inverter is working in stand alone mode and it is disconnected from any other external voltage source, this voltage source is either being a main utility grid or second inverter connected in parallel. Therefore the voltage across the end terminals of the filter (which is shown as V_g in figure 3.12) will be equal to V_0, it means the voltage across the end terminals will be the same as the voltage across filter capacitor. When the inverter is connected in parallel to the grid or second inverter then the grid side inductance L_g is used for the decoupling of inverter output voltage and grid voltage. While the grid voltage is mostly considered as a source of disturbance due to continuous variations and discontinuity in load home appliances.

By using this assumption in Eq. (3.29)

$$(sL_g + R_g)I_0 = V_0 \tag{3.30}$$

Now put the value of V_0 from Eq. (3.28)

$$\left(\frac{1}{sC} + R_c\right) I_c = (sL_g + R_g)I_0 \tag{3.31}$$

Rearranging the Eq. (3.16) and substituting the values of V_l and V_0 from Eq. (3.27) and (3.30) respectively.

$$V_{inv} = V_0 + V_l \tag{3.32}$$

$$V_{inv} = (sL_g + R_g)I_0 + (sL_i + R_i)I_i \tag{3.33}$$

$$V_{inv} = (sL_g + R_g)(I_i - I_c) + (sL_i + R_i)I_i \tag{3.34}$$

$$V_{inv} = (sL_g + R_g)(I_i) - (sL_g + R_g)(I_c) + (sL_i + R_i)I_i \tag{3.35}$$

From Eq. (3.31)

$$\left(\frac{1}{sC} + R_c\right) I_c = (sL_g + R_g)(I_i - I_c) \tag{3.36}$$

After rearranging Eq. (3.36)

$$(sL_g + R_g)(I_i) = \left(\frac{1}{sC} + R_c\right) I_c + (sL_g + R_g)(I_c) \tag{3.37}$$

Solution of Eq. (3.37) will be

$$I_c = \left(\frac{s^2 L_g C + sCR_g}{s^2 L_g C + sC(R_g + R_c) + 1}\right) I_i \tag{3.38}$$

Now substitute the value of I_c into Eq. (3.35)

$$V_{inv} = (sL_g + R_g)(I_i) - (sL_g + R_g)\left(\frac{s^2 L_g C + sCR_g}{s^2 L_g C + sC(R_g + R_c) + 1}\right) I_i + (sL_i + R_i) I_i \tag{3.39}$$

Solution of Eq. (3.39) will be given in Eq. (3.41) For the sake of a simple equation lets use following notations:

$R_{eq} = R_c R_g + R_c R_i + R_g R_i$

$R_z = R_g + R_i$

$$G_i(s) = \frac{I_i(s)}{V_{inv}(s)} \tag{3.40}$$

$$G_i(s) = \frac{s^2 L_g C + sC(R_g + R_c) + 1}{s^3 C(L_g^2 + L_i L_g) + s^2 C(L_g(R_c + R_i) + L_i(R_c + R_g)) + s(L_g + L_i + C(R_{eq})) + R_z} \tag{3.41}$$

This is the transfer function from V_{inv} to I_I which is inverter inductor current, this transfer function will be used to tune the current controller of the inner control loop.

Let's develop another transfer function from V_{inv} to V_0.

From Eq. (3.16)

$$V_{inv} = V_l + V_0 \tag{3.42}$$

Put the values of V_0 and V_l

$$V_{inv} = (sL_i + R_i)I_i + \left(\frac{1}{sC} + R_c\right) I_c \tag{3.43}$$

From Eq. (3.15) put the value of I_i

$$V_{inv} = (sL_i + R_i)(I_c + I_0) + \left(\frac{1}{sC} + R_c\right) I_c \tag{3.44}$$

Put the values of I_c and I_0 by using Eq. (3.28) and (3.30) respectively

$$V_{inv} = (sL_i + R_i)\left(V_0 sC + \frac{V_0}{sL_g + R_g}\right) + \left(\frac{1}{sC} + R_c\right) V_0 sC \tag{3.45}$$

By solving Eq.(3.45)

$$V_{inv} = \left(\frac{s^3 CL_iL_g + s^2C(L_g(R_c + R_i) + L_iR_g) + s(L_g + L_i + C(R_iR_g + R_gR_c)) + R_i + R_g}{sL_g + R_g}\right) V_0 \tag{3.46}$$

So the Second transfer function will be

$$G_v(s) = \frac{V_0(s)}{V_{inv}(s)} \tag{3.47}$$

$$G_v(s) = \frac{sL_g + R_g}{s^3 CL_iL_g + s^2C(L_g(R_c + R_i) + L_iR_g) + s(L_g + L_i + C(R_iR_g + R_gR_c)) + R_i + R_g} \tag{3.48}$$

This is the transfer function from V_{inv} to V_0 which is an output voltage of the plant, this transfer function will be used to tune a voltage controller of the inner control loop.

3.5 Droop Control

Droop control is the main part to which this thesis work is contributing. A completely new droop control technique has been proposed to improve the stability of the system. A new control technique which is developed during this thesis work uses an online estimation technique while other researchers are more focusing on adaptive and robust techniques. Some of the advanced techniques which have been developed by other researchers are mentioned in section 3.1.3 with the introduction of droop control method.

Different tools which have already been developed are used together in a new combination or topology to achieve a successful estimation of droop gains. This online estimation technique has not yet been used by any other researcher. In next sections this new methodology will be discussed step by step. This technique will make the system more reliable and reduces the calculations needed either before or during the inverter operations. This section will discuss the mathematical modelling of droop control and estimation of droop coefficients. The main purpose of the droop control is to generate a reference signal for inner control loop which consists of voltage and current controller with relatively higher bandwidth than droop or power control block. This droop control block which is also known as the power control block is the outer most control block with low bandwidth as compared to inner control loop (voltage and current controller). There are two reasons for this choice:

1. In a grid connected mode inverters are responsible to ensure the high quality power injection. Therefore the power control loop should have a slow changing reference signal for inner control loop at the output [2].

2. The output low pass filter after instantaneous power calculation block to extract average power components should have low cut off frequencies as shown in figure 3.5. In a result this outermost control loop will have bandwidth in the range of 2 to 10Hz [2].

There are three main stages of the proposed droop control scheme as shown in figure 3.13.

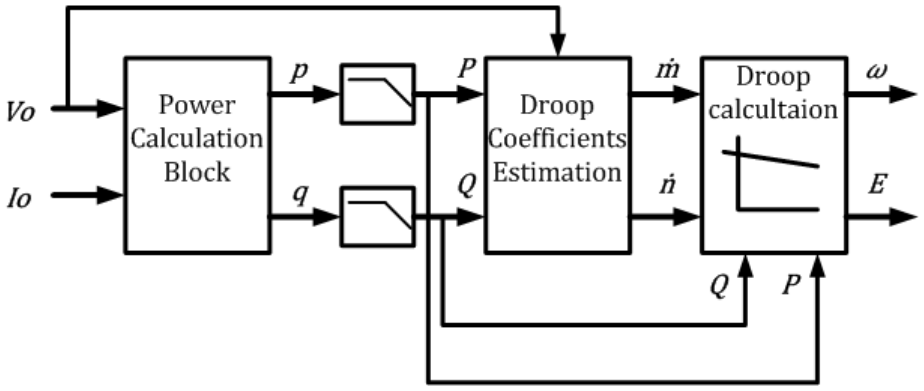

FIGURE 3.13: Estimated Droop control scheme

1. Power calculation block which has output voltage V_0 and output current I_0 as input signals. This block gives active power P and reactive power Q as outputs, which are used for droop coefficients estimation and droop control.

2. Droop estimation block which has active power, reactive power and output voltage as inputs, which results in estimated droop coefficients.

3. Droop curve implementation and reference signal generation.

3.5.1 Power Calculation block

This block needs two orthogonal components of space vectors. In three phase system these orthogonal components can be generated either by using Clarke's transformation or Park's transformations. Since the system which is used in this thesis work is a single phase inverter therefore a new method is required. In section 3.3.1 solution to this problem has already been proposed named as second order generalized integrator. This method is successfully used in [31, 38, 39].

These orthogonal components (through transfer functions given in Eq. (3.8) and (3.9)) can be used as follows for the calculation of active and reactive power:

$$v_\alpha = G_e(s)V_0 \tag{3.49}$$

$$v_\alpha = \frac{Ks}{s^2 + Ks + \omega^2}V_0 \tag{3.50}$$

$$v_\beta = G_f(s)V_0 \tag{3.51}$$

$$v_\beta = \frac{K\omega}{s^2 + Ks + \omega^2}V_0 \tag{3.52}$$

$$i_\alpha = G_e(s)I_0 \tag{3.53}$$

$$i_\alpha = \frac{Ks}{s^2 + Ks + \omega^2}I_0 \tag{3.54}$$

$$i_\beta = G_f(s)I_0 \tag{3.55}$$

$$i_\beta = \frac{K\omega}{s^2 + Ks + \omega^2}I_0 \tag{3.56}$$

$$p = \frac{1}{2}(\overrightarrow{v} \cdot \overrightarrow{i}) = \frac{1}{2}(v_\alpha i_\alpha + v_\beta i_\beta) \tag{3.57}$$

$$q = \frac{1}{2}(-\overrightarrow{v} \times \overrightarrow{i}) = \frac{1}{2}(v_\beta i_\alpha - v_\alpha i_\beta) \tag{3.58}$$

For further study lets have a time domain analysis. Inverter output voltage and current are given by

$$V_0 = \sqrt{2}V\cos(\omega t) \tag{3.59}$$

$$I_0 = \sqrt{2}I\cos(\omega t - \theta) \tag{3.60}$$

Where V and I are the rms values of voltage and current respectively ω is the fundamental frequency and θ is the angle difference between voltage and current. So the instantaneous active and reactive power delivered by the inverter is given by

$$p = V_0 I_0 = VI\cos(\theta) + VI\cos(2\omega t - \theta) \tag{3.61}$$

$$q = V_0 \perp I_0 = VI\sin(\theta) + VI\sin(2\omega t - \theta) \tag{3.62}$$

From Eq. (3.61) and (3.62) it can be seen that both active and reactive powers have two components. One is an average value of active and reactive power while the second part is showing oscillatory nature with double frequency. A first order low pass filter is being used to filter out this double frequency component so that an average active and reactive power can be obtained for further use in droop control block.

$$P = \frac{\omega_c}{s + \omega_c} p \tag{3.63}$$

$$Q = \frac{\omega_c}{s + \omega_c} q \tag{3.64}$$

Where ω_c is the cutoff frequency. Usually the value of cutoff frequency ω_c is kept one decade lower than the fundamental frequency ω [38].

3.5.2 Estimation Block

This has already been stated that this thesis work is proposing a new droop control technique known as estimated droop control. This estimation block differentiates this thesis work and its technique from the work of other researchers. Couple of estimation techniques which have already been developed for SOGI, PLL or some other tool boxes

by researchers are used in a new combination to estimate droop gains. This has been ensured that this new combination will not affect the system and will give optimal performance with best possible error rejection capability. This section will present this proposed methodology and modelling in detail.

There are three input signals, output voltage V_0, active power P and reactive power Q. This block uses the combination of SOGI with Kalman gains and phase locked loop (PLL). Droop coefficients are very important parameters so they should be estimated very precisely with minimum chance of error. Therefore best possible way of estimation is through the Kalman filter to make system as much precise as possible.

So orthogonal components are estimated by using the transfer functions in Eq. (3.10) and (3.11) as follows:

$$\hat{v}_\alpha = \frac{k_1 s - k_2 \omega}{s^2 + k_1 s + \omega^2 - k_2 \omega} V_0 \tag{3.65}$$

$$\hat{v}_\beta = \frac{k_2 s + k_1 \omega}{s^2 + k_1 s + \omega^2 - k_2 \omega} V_0 \tag{3.66}$$

Equivalent PLL model of implemented model shown in figure 3.11 is given in figure 3.14. In this figure $\theta^* = \hat{\theta}$

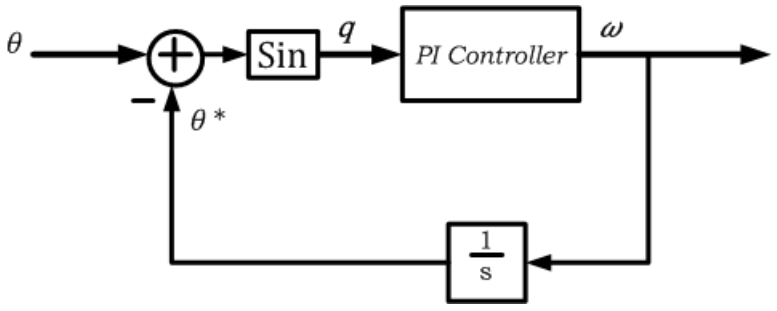

FIGURE 3.14: Equivalent Phase Locked Loop

$$q = \hat{u}_\beta \cos(\hat{\theta}) - \hat{u}_\alpha \sin(\hat{\theta}) \tag{3.67}$$

By using trigonometric properties for Eq. (3.65) and (3.66), then put the values of v_α and v_β in Eq. (3.67)

$$q = (\sin(\theta)\cos(\hat{\theta}) - \cos(\theta)\sin(\hat{\theta}))V_0 \tag{3.68}$$

$$q = \sin(\theta - \hat{\theta})V_0 \tag{3.69}$$

when the between θ and $\hat{\theta}$ is small then $\sin(\theta - \hat{\theta}) \approx \theta - \hat{\theta}$

$$\hat{\omega} = \sin(\theta - \hat{\theta}) V_0 \frac{K_p s + K_i}{s^2 + V_0 K_p s + V_0 K_i} \tag{3.70}$$

Where K_p and K_i are proportional and integral gains of PI controller respectively.

$$\hat{\theta} = \int \hat{\omega} dt \tag{3.71}$$

Furthermore these estimated orthogonal output components can also be used to calculate absolute peak value of an input sinusoidal signal [31]. A definition of space vector is used for calculation of peak value [31].

$$\hat{E} = \sqrt{\hat{v}_\alpha^2 + \hat{v}_\beta^2} \tag{3.72}$$

RMS value can be calculated as follow:

$$\hat{V}_{RMS} = \frac{\hat{E}}{\sqrt{2}} \tag{3.73}$$

Now two main parameters $\hat{E}$ peak value of output voltage from Eq. (3.73) and $\hat{\omega}$ angular frequency from Eq. (3.70) has been estimated. These parameters are further used for the estimation of droop coefficients. Before starting with the estimation of droop coefficients, there are two other parameters need to know ϵ_p and ϵ_q. These two parameters belong to frequency and voltage droop tolerance respectively. It has been observed that during coefficient estimation, system encounters with singularity. Therefore to avoid this singularity a pivot with a small value is added with active and reactive power.

$$\overline{P} = P + \xi \tag{3.74}$$

$$\overline{Q} = Q + \xi \tag{3.75}$$

$$\hat{m} = \frac{\hat{\omega}\epsilon_p}{\overline{P}} \tag{3.76}$$

$$\hat{n} = \frac{\hat{E}\epsilon_q}{\overline{Q}} \tag{3.77}$$

3.5.3 Droop Curve

New droop curve equations will be like this:

$$\omega = \omega^* - \hat{m}P \tag{3.78}$$

$$E = E^* - \hat{n}Q \tag{3.79}$$

In traditional droop control, values of droop coefficients are fixed. These values are calculated based on rated apparent power S_{max}, desired frequency and output voltage. These values cannot be updated if there is a change in inverter operations or output values. Inverter continue using these old and fixed values, so this is most likely to make a system unstable if there are severe variations in system parameters. In next chapter different operating conditions will be discussed and explained.

With online estimated values for droop coefficients it is possible to adopt new values for droop coefficients if there is any deviation from normal circumstances happening. This technique gives more robustness and reliability in system operation.

Now ω and E from Eq. (3.79) and (3.80) respectively will be used to generate a tracking signal for inner control loops.

$$\varphi = \int \omega dt \tag{3.80}$$

$$V_{ref} = E \sin \varphi \tag{3.81}$$

Where V_{ref} is a reference or tracking signal for inner control loop

3.6 Inner Control Loop

This control loop usually consists of two control units one is voltage control and the second is current control. If the grid is operating with stiff voltage then there is no need for voltage regulation. If the grid is weak and the voltage stiffness is low then voltage regulation is needed and this is critical for high quality power injection. Most of the microgrids based on renewable energy sources have low voltage stiffness, therefore they need voltage regulation.

Similarly a current controller is responsible for the characteristics of injected current. It is highly desirable that inverter current should be free from low order harmonics. While high frequency harmonics can be eliminated by using grid - side filters.

These two control units play a very important role in the stability and effectiveness of a DG unit. In following subsections these two control units will be discussed in detail and block diagram of the inner control loop is shown in figure 3.15.

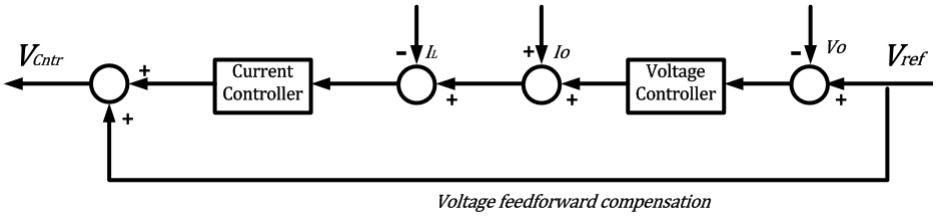

FIGURE 3.15: Inner control loop

3.6.1 Voltage control

Voltage control unit can be used in two conditions when voltage regulation is needed in a grid connected mode where the grid has low voltage stiffness. Secondly in an island mode where the DG units are connected near the sensitive loads and high voltage quality is needed [2]. In island mode power quality is also determined by the inverter output voltage. There should be low total harmonic distortion (THD) under different load conditions because harmonic distortion in current due to non-linear load can easily affect the output voltage of the inverter. There should be fast recovery in case of load variation and disturbances in networks with low voltage dip [2].

3.6.2 Current Control

The current control unit is responsible for injecting current. In VSI based DG units current control units are applied with high bandwidth to have accurate current tracking normally 10 times higher bandwidth than voltage control unit [38] and also to have fast transient response as much as possible. Recent investigations have shown that small disturbances in grid voltage can increase THD level in injected current which can lead inverter system to instability. So the current control unit should be fully capable to deal with grid side disturbances.

3.6.3 Proportional Integral and Proportional Resonant Controller

These proportional integral (PI) controllers were very popular in the design of inverter and still are in use. These linear PI controllers have to handle non-linear errors. It is difficult to tune these PI controllers to achieve desired regulation for fundamental frequency and output voltage. Since the PI controller has a pole at zero so it cannot give fast dynamic response against sudden disturbances. Performance of PI controller is also poor against lower order harmonics. Another disadvantage of PI controller is a steady state phase error (integral part introduces a phase lag which may cause instability) and its sensitivity towards system parameters [2, 47]. The transfer function of a PI controller is given as follows:

$$G_{PI}(s) = K_p + \frac{K_i}{s} \tag{3.82}$$

Proportional resonant (PR) controller is getting more popular in inverter design because of its better performance as compared to PI controller. A PR controller gives a high gain at fundamental frequency which improves its functionality for the rejection of low order harmonics. PR controller is also useful for mitigating grid harmonics which can affect the performance of a current controller. The transfer function of a PR controller is given as follows:

$$G_{PR}(s) = K_p + \frac{K_i s}{s^2 + \omega^2} \tag{3.83}$$

Where ω is the resonant frequency. A PR controller has very high gain around the resonant frequency therefore it can eliminate steady state error. The bandwidth of a PR controller depends on the value of K_I [38, 47–49].

Normally the purpose of the controller and the process structure determines which configuration of PID controller can be used to control the system. As Proportional part (P) is used to speed up the controller response, Integral part (I) is used to eliminate the steady state error and Derivative part (D) is used to stabilize the control system but also make the controller more sensitive to noise or disturbances. Due to this sensitivity of derivative part, researchers avoid to use PID controller in inverter design because the output voltage will always be subject to different kind of disturbances and fluctuations. The power distribution network always has disturbances due to bad weather like thundering or continuous change in load demand because of different kinds of commercial and home appliances and their collective effect upon the main power system.

3.7 Tuning of Controllers

This thesis has used PR controller, this section will discuss how a PR controller has been tuned for best possible results. Different methods have been used for the tuning of controllers. The process which is used to obtain the suitable gains for the controller is called tuning of the controller. Tuning methods that has been used in this thesis work are given by

1. Ziegler-Nichols Method
2. Chien Hrones-Reswick Method
3. Robust Response time Method

Two very important tuning methods were published in 1942 by John G. Ziegler and Nathaniel B. Nichols, these method to combine are known as Ziegler-Nichols method. This method tends to give fast step response without excessive oscillations and with good disturbance rejection property [50]. There are two methods which are being used to tune Ziegler-Nichols controller one is based on the closed loop concept which needs maximum gain and maximum time period of a wave oscillating with constant amplitude. The other method based on the open loop concept which requires a general step response of the system. The main advantage of this method is that it does not require a very precise model for tuning, an assumed model can also give accurate results which make this method very practical for process control applications. Therefore Ziegler-Nichols method is a good choice to proceed with it, anyhow final decision will be made after analysing the response of different tuning methods. Detail explanation can be found in [50, 51].

Chien Hrones-Reswick method was developed to improve the quality of open loop system performance. This controller can be tuned with set-point regulation or with disturbance rejection property. This control was derived from Ziegler-Nichols method [51]. This tuning method is capable to accommodate both response speed and overshoot. The detailed design procedure is explained in [51].

The robust response time method gives more freedom in design. This method allows to choose bandwidth and phase margin as per requirement. Gains are tuned according to set bandwidth and phase margins.

The tuning of controller through all three above mentioned methods is performed and summarized in table 3.1. The choice tuning method will be made in the next chapter during the detail analysis of the system and according to the given design specifications.

TABLE 3.1: Results through different tuning methods

	Gain Margin (dB)	Phase Margin (deg)	Bandwidth (rad/sec)	Rise Time(sec)	Settling Time(sec)	Steady State Value
Ziegler Nichols Method for $G_v(s)$	12.5	44	7.44×10^3	0.00237	0.00529	1
Ziegler Nichols Method for $G_i(s)$	Inf	53.9	9.16×10^4	1.88×10^{-5}	0.000156	1
Chien Hrones Reswick Method for $G_v(s)$	12.3	43.8	7.43×10^3	0.000324	0.00613	0.881
Chien Hrones Reswick Method for $G_i(s)$	Inf	53.5	9.173×10^3	0.000313	0.0026	1
Robust Response Time Method for $G_v(s)$	18.6	59.8	7.27×10^3	0.00136	0.00422	0.999
Robust Response Time Method for $G_i(s)$	Inf	74	5.46×10^4	3.33×10^{-5}	0.000402	1

Chapter 4

Model Analysis and Simulation Results

After complete description of all the main units of inverters, this chapter will analyse the stability of a model. A general concept of stability is that a system has a bounded output in the response of a bounded input. An open loop system may or may not be stable. If an open loop system is not stable, a feedback compensation can be used to make it stable and suitable control parameters can be used to adjust the transient response of the system. If open loop system is stable, a feedback compensation can be used to improve the stability level of the system. If a close loop system is stable then a term "*relative stability*" is used to measure the degree of stability [50]. It is necessary to discuss the stability through different techniques.

Techniques that have been used in this work are as follows:

1. Pole-Zero mapping
2. Step response (Time domain analysis)
3. Frequency domain analysis

The model analysis has been carried out for two situations which are:

1. Model analysis without Controller
2. Model analysis with Controller

4.1 Model Analysis without Controller

First of all, system analysis has been performed without controllers. This analysis is important to see how much efficient controller is needed for the desired level of performance. It will also help to analyse the behaviour of the dominant poles.

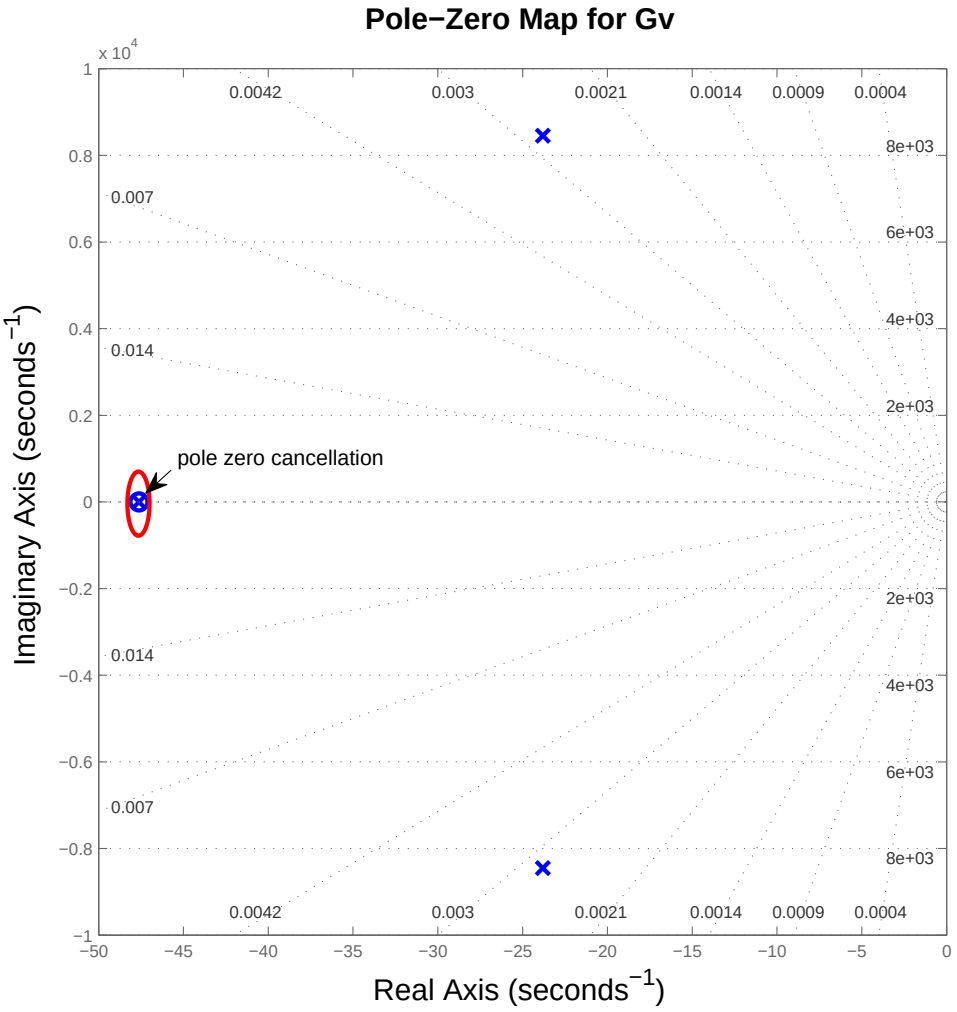

FIGURE 4.1: Pole Zero plot of transfer function $G_v(s)$

4.1.1 Pole Zero map of Voltage and Current transfer functions

In figure 4.1 a pole zero plotting for G_v is shown, poles by cross (X) and zeros by circle (o). It can be seen from figure 4.1 that there are three poles and one zero and all lie in the negative half of the *s-plane*. It can also be seen that a system has one pole zero cancellation, after that system only left with a conjugate pair of two poles with high

the value of imaginary part and comparatively a small value of real part. It is obvious from figure 4.1 that these poles are close to the origin and have oscillatory behaviour due to the less damping ration by high values of their imaginary part. Being near to the origin affect of these poles (which reflect in the form of oscillations) will decay slowly. The system will show oscillatory response when the reference signal goes from zero to a steady state value. Similarly, these poles can compromise the system stability if the disturbance is more than expected level due to their slow response.

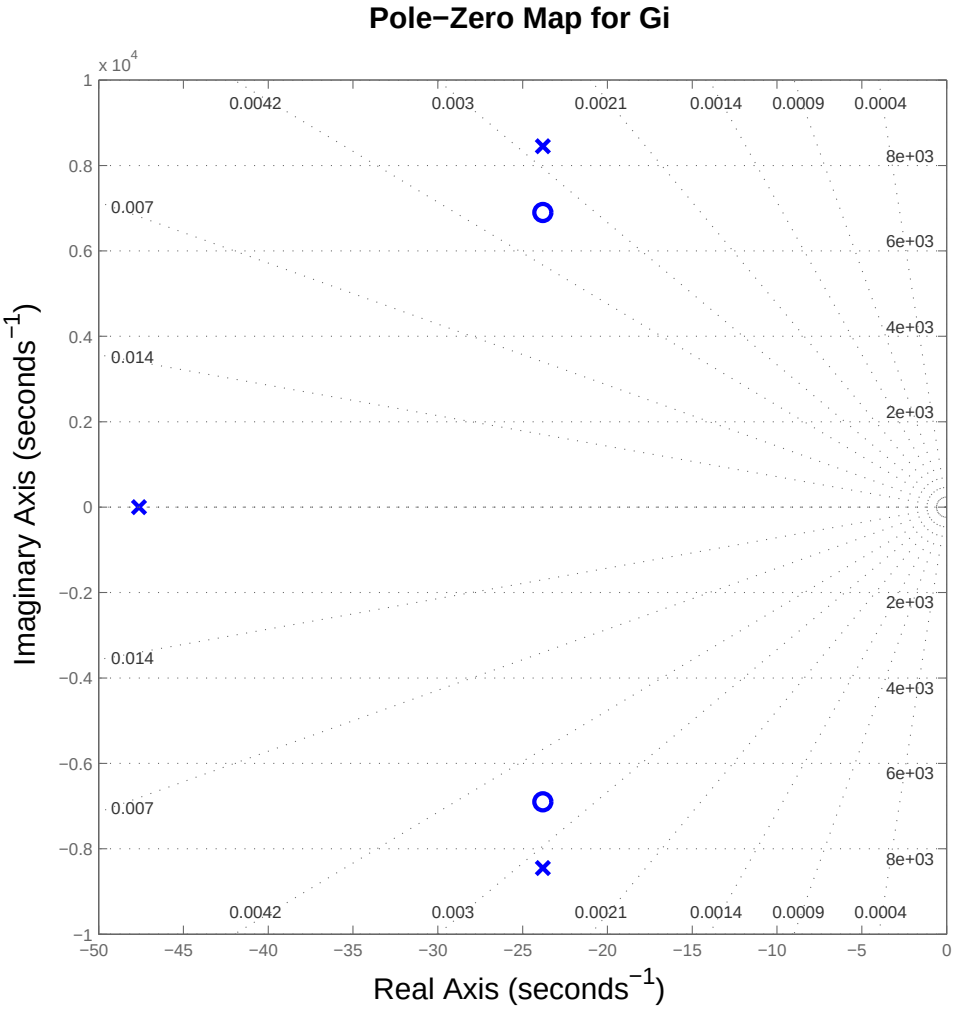

FIGURE 4.2: Pole Zero plot of transfer function $G_i(s)$

In figure 4.2 the pole zero map for transfer function G_i is shown, poles by cross (X) and zeros by circle (o). It can be seen that a system has three poles and two zeros in the negative half of the *s-plane*. It is a well known theory that the speed of the system response is dictated by the value of the real part. If the value of the real part is high, then the system response will be faster and slower for small values. While the

imaginary part dictate the damping ratio in the system response. If the poles lie on the horizontal axis, which means poles have only real part then the system will show smooth transient response without oscillations. An exponentially decaying response where the speed of this decay depends on the location of the pole. In figure 4.2 it can be seen that there is a conjugate pair of two dominating zeros with a conjugate pair of two dominating poles. These zeros and poles are dominating because they are close to origin and can influence the system response more than any other pole or zero. The additional conjugate pair of two zeros can have two effects on system response one is an overshoot due to their dominant location in pole zero map and secondly the response speed of a system increases as zeros move from $+\infty$ to 0.

4.1.2 Bode Diagrams of Voltage and Current transfer functions

Bode plot of an uncompensated voltage transfer function is shown in figure 4.3. It can be seen from figure 4.3 that resonant peak is high at the resonant frequency. The resonant frequency is given by

$$\omega_{res} = \sqrt{\frac{L_i + L_g}{L_i L_g C_f}} = 8452 rad/sec \tag{4.1}$$

This filter transfer function has $-40dB/decade$ gain after resonant frequency and has almost $-10dB$ gain at fundamental frequency $\omega_0 = 314 rad/sec$. Gain Margin is infinity and Phase Margin is $4.48deg$.

Bode plot of an uncompensated transfer function $G_i(s)$ is shown in figure 4.4. The system has $-40dB/decade$ gain after resonant frequency and around $-32db$ gain at the fundamental frequency. Both Gain Margin and Phase Margin are *infinity*.

4.2 Design Specifications

In the last section an initial analysis has been performed for voltage and current transfer functions. From pole zero plots of both voltage and current transfer functions, it is obvious from figure 4.1 and 4.2 (for G_v and G_i respectively) that system is stable but improvements are needed. From bode plots in figure 4.3 and 4.4 for G_v and G_i respectively, it can be assumed that a system either has very a low robustness or poor stability margins.

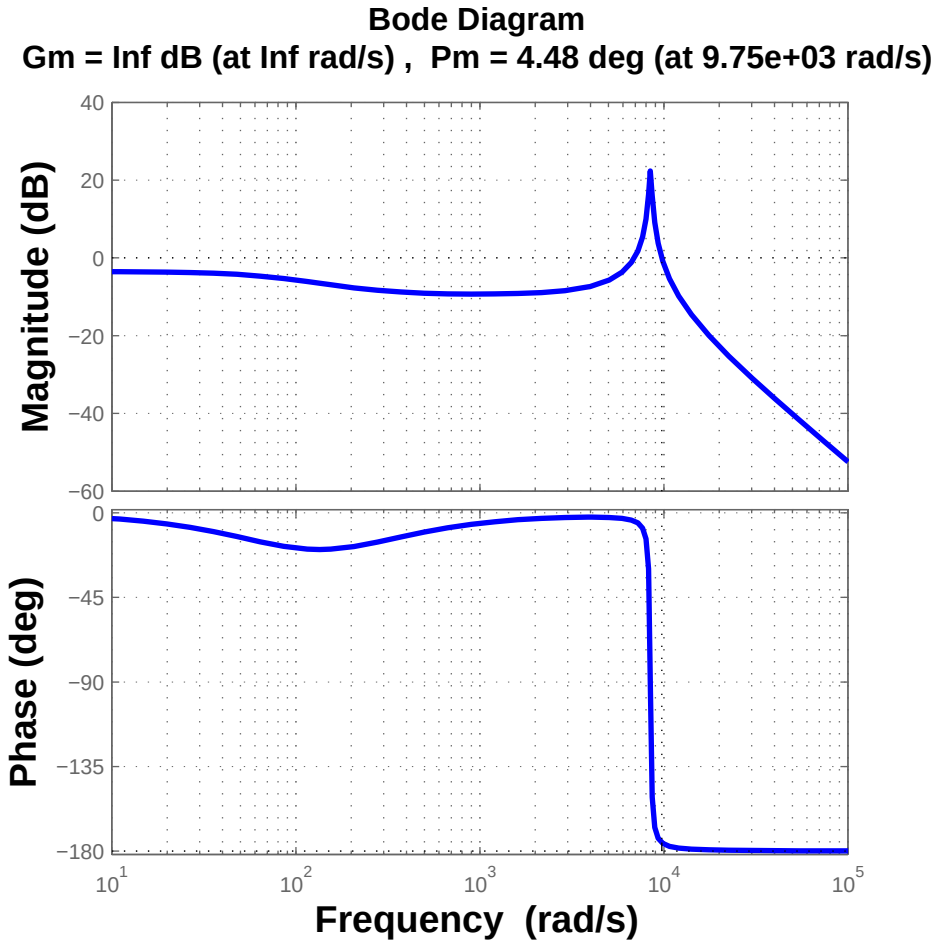

FIGURE 4.3: Bode plot of transfer function $G_v(s)$

Transfer functions given in Eq. (3.48) and (3.41) are used for tuning voltage and current controller respectively. Following specifications have been set to improve the relative stability and performance of the system:

1. Gaim margin should be greater than $10dB$.
2. Phase margin should be greater than 40^o.
3. Bandwidth of current controller should be greater than Bandwidth of voltage controller.
4. Zero steady state error at the fundamental frequency (ω=$314rad/sec$).

Before starting with the design specifications given above, let's define a few important terms which may help in understanding bode plots.

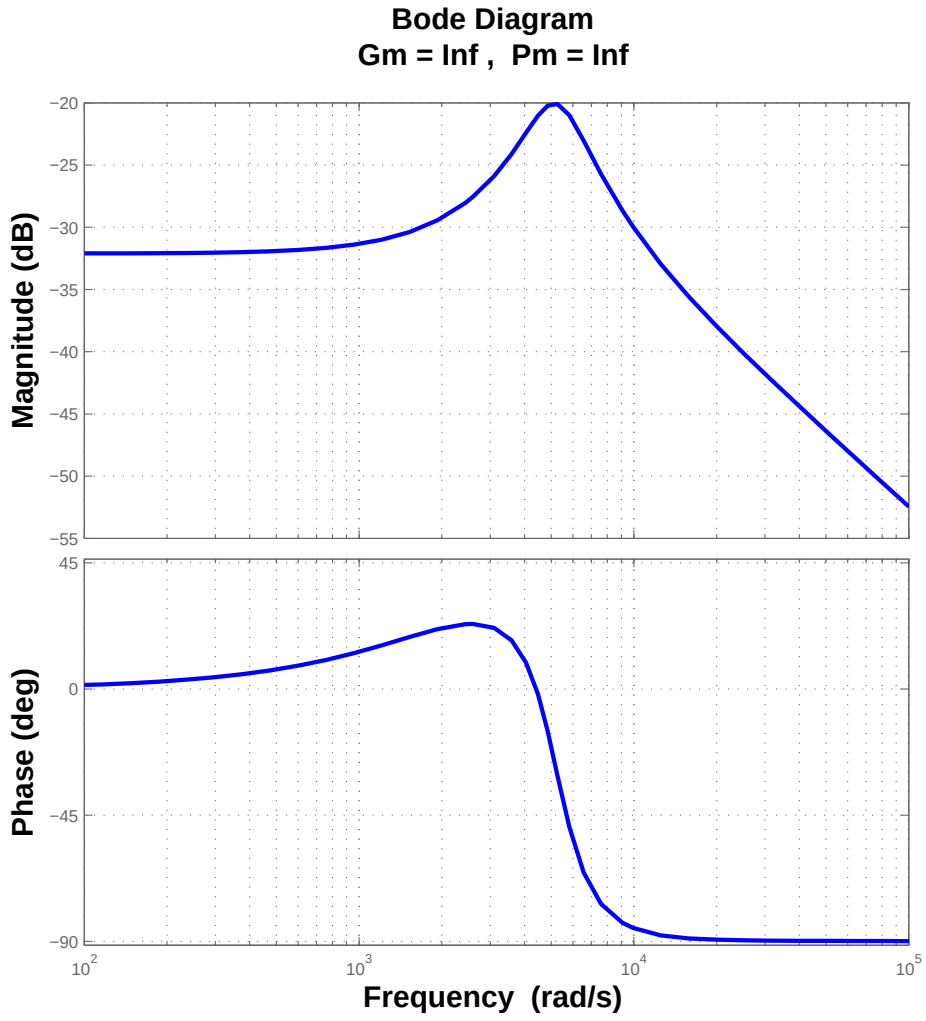

FIGURE 4.4: Bode plot of transfer function $G_i(s)$

Gain margin measures how much variation in gain can be tolerated before the system become unstable at the phase crossover frequency (frequency at which phase response curve is at $-180deg$ or crosses $-180deg$).

Phase margin measures how much variation in phase can be tolerated before system become unstable at a gain crossover frequency (frequency at which the gain curve of the system is at $0dB$ or crosses the $0dB$ gain line).

Bandwidth of a system is the measure of frequency after resonant frequency at which magnitude curve has $-3dB$ gain in the close loop system. Bandwidth is also related to the quick response of a system, the much higher the bandwidth of a system the much faster the response of a system would be. System with high bandwidth show better performance in terms of reference tracking and achieving desired steady state value [50].

4.3 Model Analysis with Controller

In figure 4.3 and 4.4 both plots are without any compensation for $G_v(s)$ and $G_i(s)$. To find a suitable compensation for these two systems, there is a need to tune the system. In figures 4.5 and 4.6 bode plots of both output voltage and current transfer functions has been shown respectively.

4.3.1 Bode Diagrams of Voltage and Current transfer functions with Controller

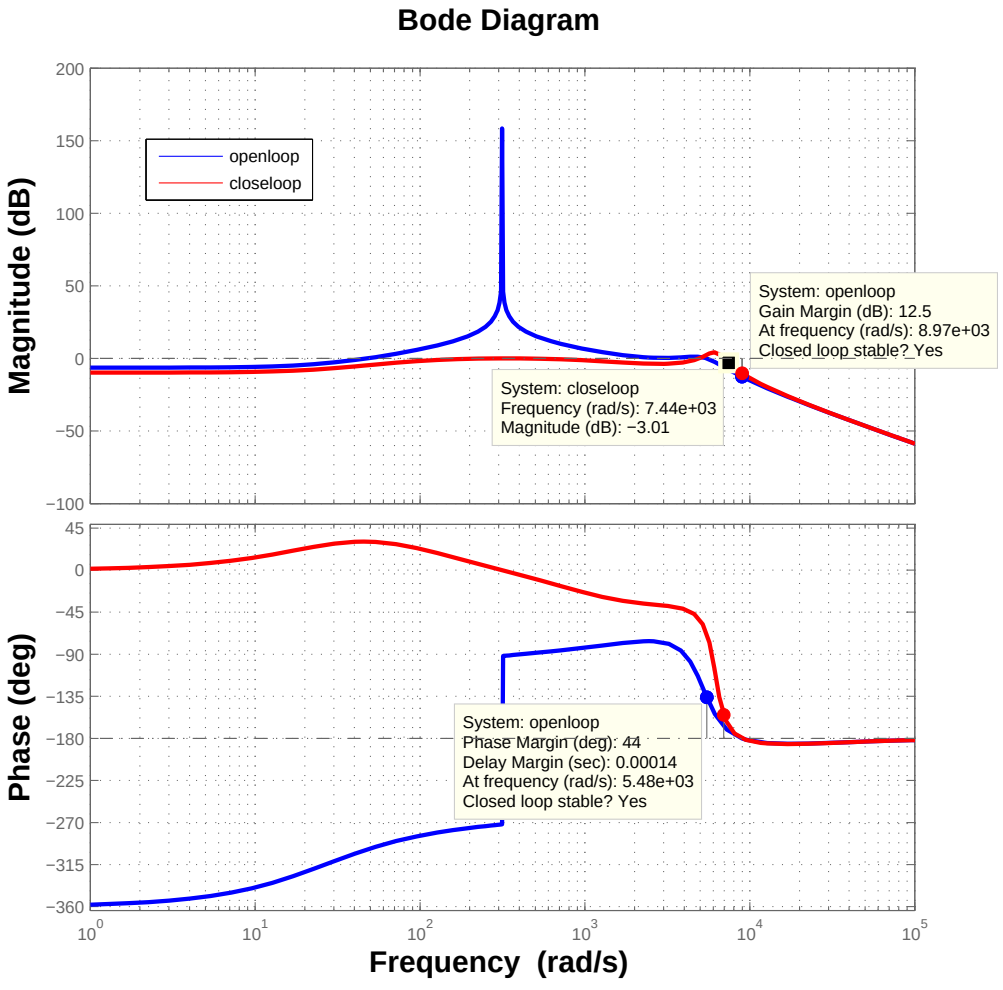

FIGURE 4.5: Bode plot of transfer function $G_v(s)$ with compensation through Ziegler-Nichols method

For $G_v(s)$ response of the system in the frequency domain with compensation through Ziegler Nichols method can be seen in figure 4.5 for both open and close loops. After the tuning of PR controller for $G_v(s)$, it will have the following gains:

$$K_p = 0.4239$$

$$K_i = 1570$$

It has been stated in [41] that proportional gain determines the speed of a system response. If this proportional gain exceed from a certain limit this can produce oscillations and these oscillations may result in an unstable system. The above mentioned proportional gain value is not very high in fact it is best possible value according to the design specifications which are listed in section 4.2. Integral gain is more concerned about the steady state error elimination [41], again unnecessarily high values can cause overshoot, oscillations or instability.

The system has high gain at fundamental frequency $\omega_0 = 314 rad/sec$ in open loop this shows characteristics of a PR controller. Gain margin is $12.5 dB$ and Phase margin is $44 deg$, while the bandwidth of the system is $7.44 \times 10^3 rad/sec$ in closed loop.

The result of a tuned current controller is shown in figure 4.6, compensation is obtained through Ziegler Nichols method. Controller gains are given as follows:

$$K_p = 521$$

$$K_I = 5.517 \times 10^7$$

It can be seen that both gain values are very higher than voltage controller. The high value of proportional gain for the current controller shows that current controller has faster response than voltage controller. Similarly integral gain is also very high which shows a strong integral effect on the system. It is stated in [38, 47–49] that integral gain is directly linked with controller bandwidth which means to increase the bandwidth of a controller, the value of an integral gain need to increase. This current controller also has high gain at the fundamental frequency, phase margin is $53.9 deg$ where as gain margin is *infinity*. The bandwidth of this current controller is $9.16 \times 10^3 rad/sec$ which is higher than voltage controller. This is in one of the desired specifications that the bandwidth of a current controller should be higher than the bandwidth of a voltage controller. Reason is that a current controller have to deal with current harmonics which are produced due to different kinds of load either linear or non-linear. Current controller with higher bandwidth has very fast response towards these disturbances.

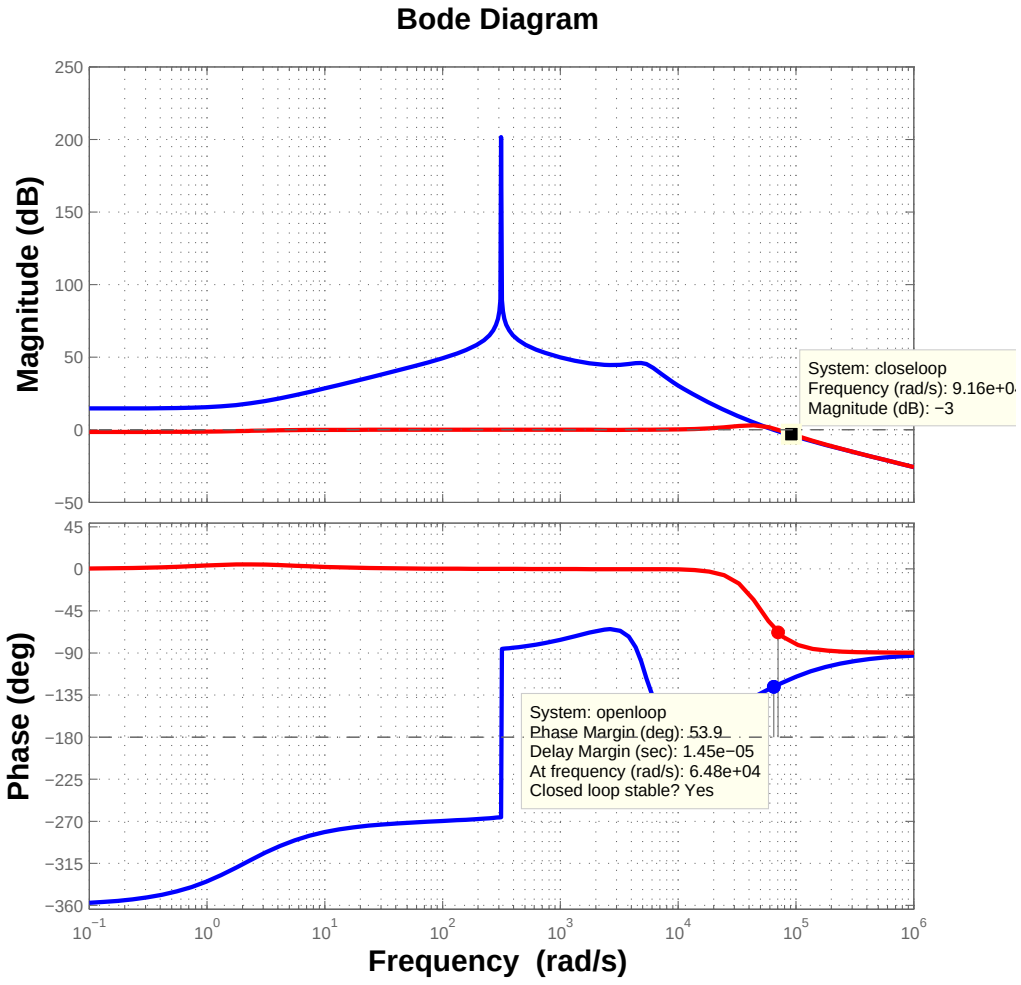

FIGURE 4.6: Bode plot of transfer function $G_i(s)$ with compensation through Ziegler-Nichols method

4.3.2 Pole Zero map of Voltage and Current transfer functions with Controller

Now a pole zero map for voltage transfer function $G_v(s)$ with controller is shown in figure 4.7. the poles of a given system are :

$$-1.6750 \times 10^4$$

$$-0.0774 + 0.6138i \times 10^4$$

$$-0.0774 - 0.6138i \times 10^4$$

$$-0.1185 \times 10^4$$

$$-0.0088 \times 10^4$$

If the poles of a compensated system in figure 4.7 are compared to the poles of an uncompensated system in figure 4.1. It can be seen that the dominant poles of G_v which may cause an oscillatory response with a slow exponential decay are moved away from the origin. It is known that the poles with high negative values have faster response as compared to those with small negative values. Likewise the imaginary part of these values also reduces which may improve the damping of the system. It can be seen that the dominant poles and zeros have real negative values which can dictate a smooth transition without any overshoot. So the poles of the system are pushed more into the left side of the *s-plane* by the controller as compared to the system without controller, this system has made relatively more stable and less oscillatory.

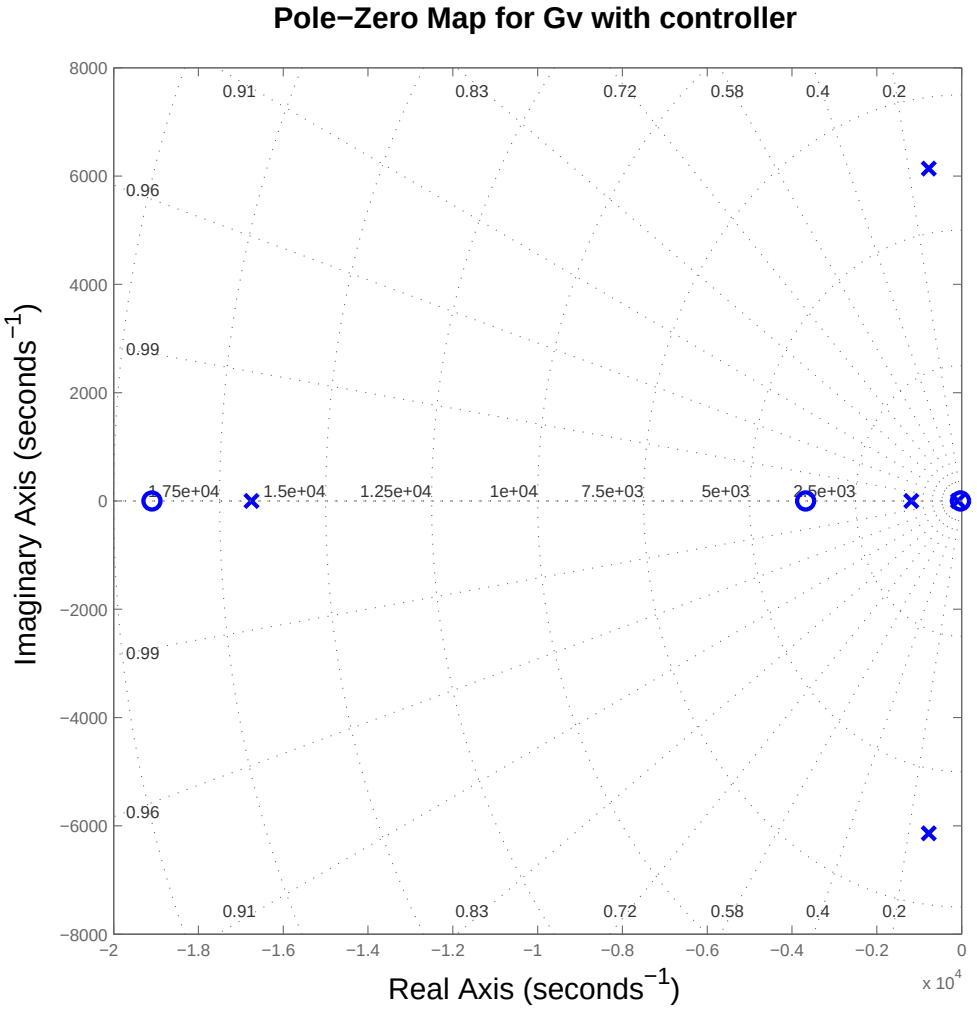

FIGURE 4.7: Pole zero plot for transfer function $G_v(s)$ with compensation through Ziegler-Nichols method

Pole zero plotting for transfer function $G_i(s)$ with current controller is shown in figure 4.8. Poles of the system are:

$$-2.6092 + 4.2628i \times 10^4$$

$$-2.6092 - 4.2628i \times 10^4$$

$$-1.6473 \times 10^4$$

$$-0.2862 \times 10^4$$

$$-0.0002 \times 10^4$$

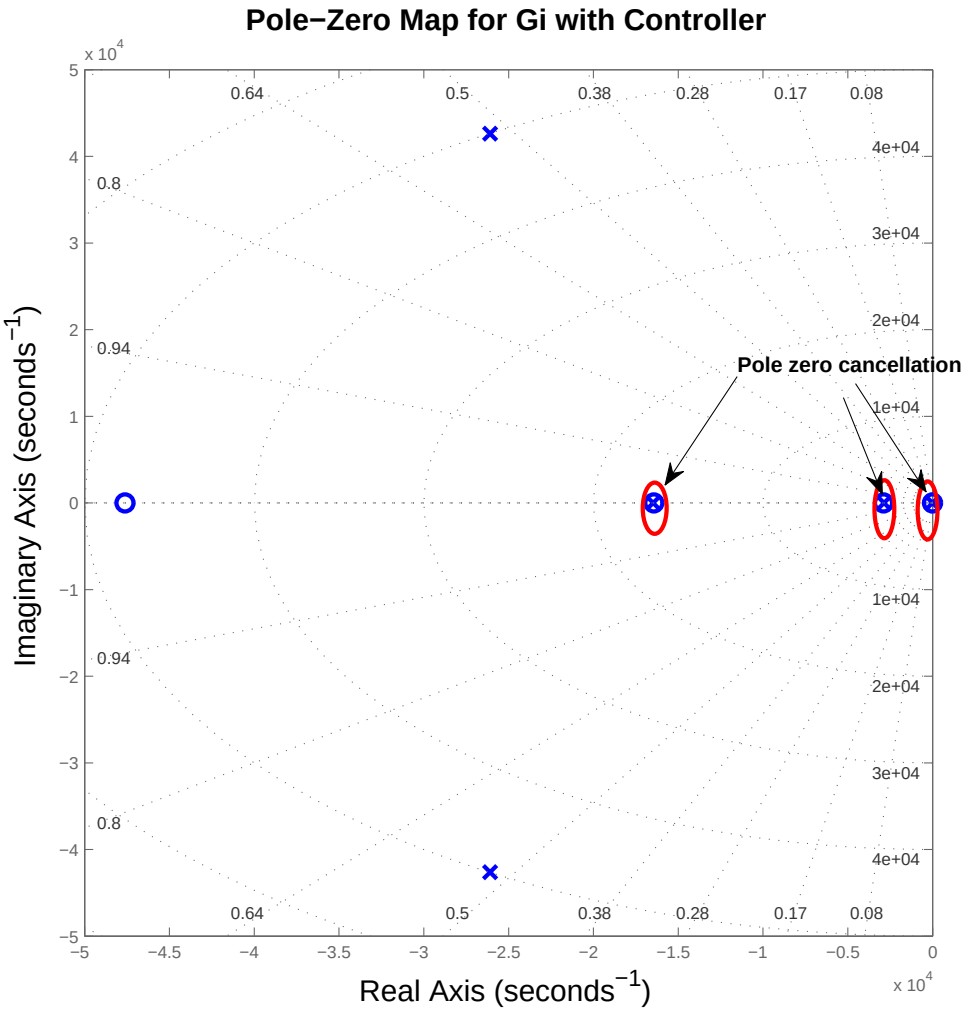

FIGURE 4.8: Pole zero plot for transfer function $G_i(s)$ with compensation through Ziegler-Nichols method

If the poles of the compensated system in figure 4.8 are compared to the poles of an uncompensated system in figure 4.2, it can be seen that the dominant poles (a conjugate pair) of the transfer function which may cause an oscillatory behaviour are pushed more towards the left. The poles far from the origin have faster response than the poles near

the origin and the oscillatory effect also decays more quickly than the poles near the origin. Now a system with the controller in figure 4.8 has three pole zero cancellation. In figure 4.2 there is a conjugate pair of two zeros, which have been settled by the controller in figure 4.8. It can also be seen that the dominant poles of the current controller in figure 4.8 are farther from the origin than the poles of the voltage controller in figure 4.7, which shows that the current controller is faster than the voltage controller. This behaviour of poles supports the statement which has been made during the frequency domain analysis through bode plot that the current controller with higher bandwidth, make it faster than the voltage controller and then by comparing the integral gain of the two controllers same argument has been presented.

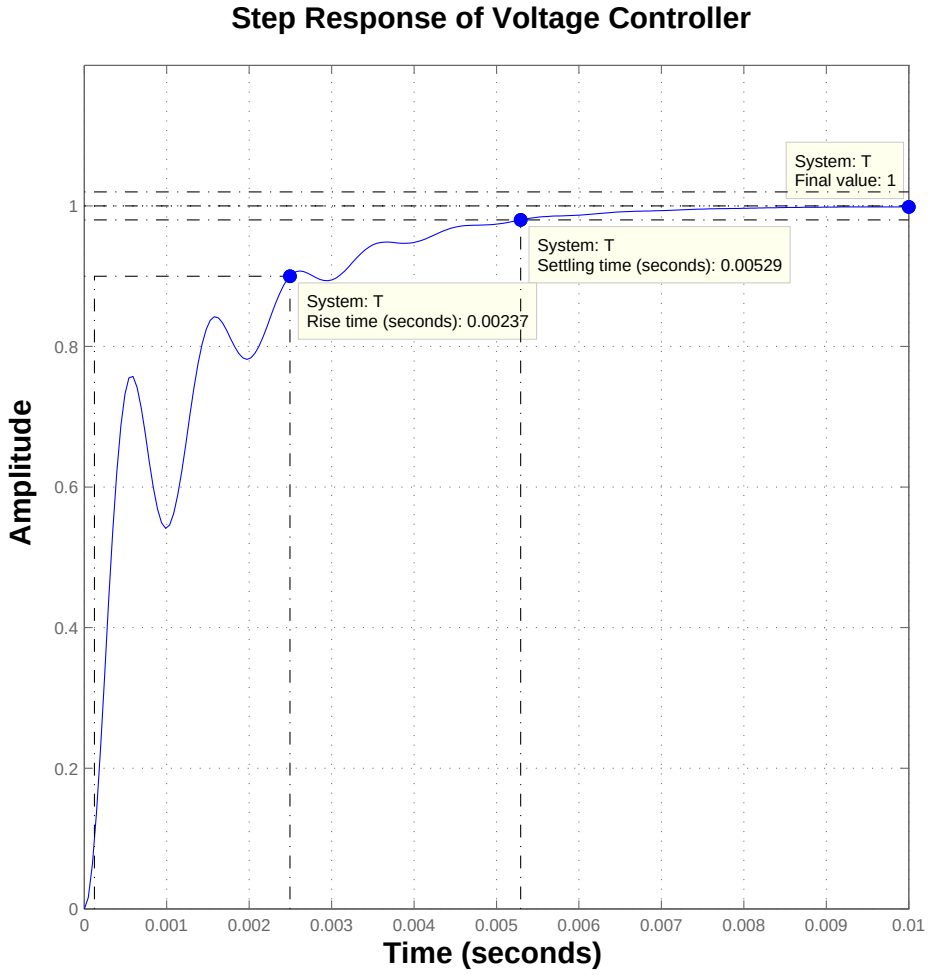

FIGURE 4.9: Step response of transfer function $G_v(s)$ with compensation through Ziegler-Nichols method

4.3.3 Step Response of Voltage and Current transfer functions with Controller

Step response is used for time domain analysis of a system. The step response for $G_v(s)$ with compensation is shown in figure 4.9, steady state value is 1 because the voltage is raised from 0 to 325V, settling time is $0.00529sec$ and the rise time is $0.00237sec$. The system does not show any overshoot and steady state error. So this time domain analysis endorse the stability in time domain.

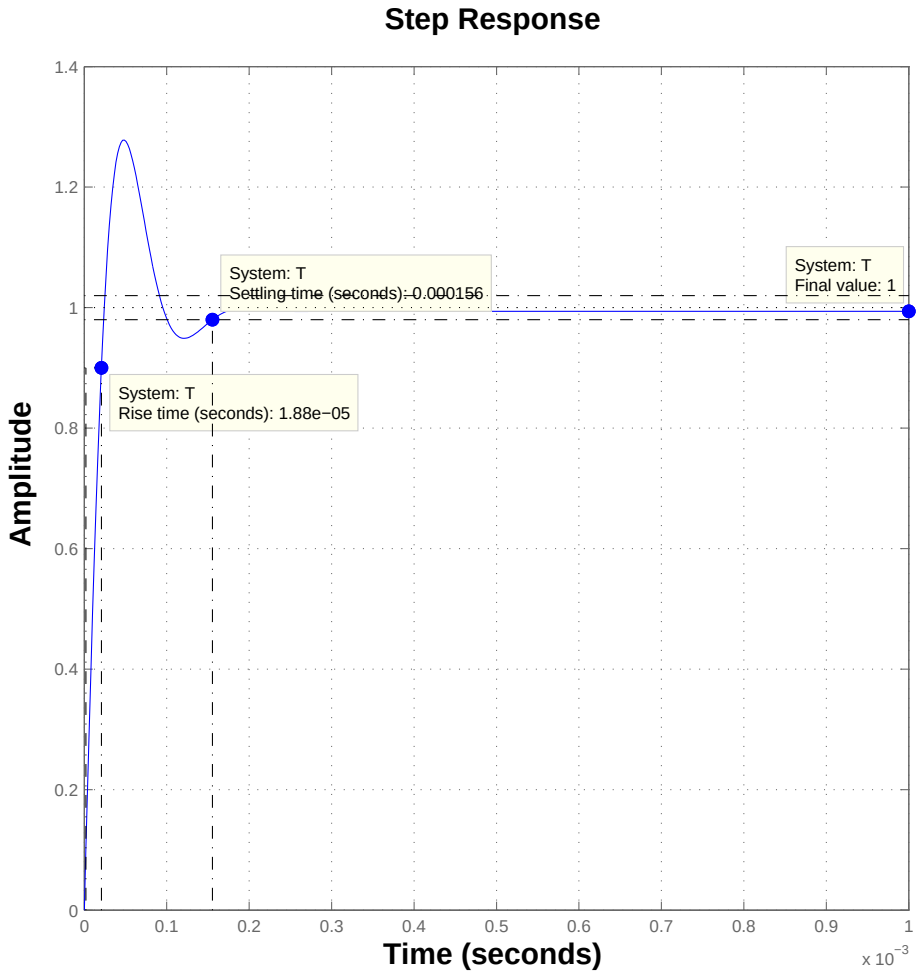

FIGURE 4.10: Step response of transfer function $G_i(s)$ with compensation through Ziegler-Nichols method

Step response of a system is shown in figure 4.10, it can be seen that the system has steady state value 1, settling time $0.000156sec$ and rise time $1.88 \times 10^{-5} sec$. This system also has 27% overshoot but zero steady state error. After comparing both voltage and current controller it can be seen that the response of current controller with compensation through Ziegler Nichols method is faster than the voltage controller. This is also

clear that a system with higher bandwidth shows faster response than a system with lower bandwidth. It can also be seen that the bandwidth of a current controller is almost 10 times higher than the bandwidth of a voltage controller.

It has been discussed earlier that three methods have been used for the tuning of voltage and current controllers. Graphs for the other two methods can be seen in **Appendix B**, while the results are summarized in table 3.1. Gain Margin for the current controller in all three methods is infinity. Gain margins and Phase margins in Ziegler Nichols method and Chiens Hrones Reswick method are almost same but there is a difference in their bandwidths. In time domain analysis they show different values for rise time and settling time. The steady state value is same for current controller but for the voltage controller steady state values are also different. In robust response time method there is a choice to select desired bandwidth and phase margin and then perform tuning of a system. Output values are nearly same to input values. Another interesting fact is all three methods giving almost same bandwidth for voltage controller. Step response analysis of voltage controller shows different values even different steady state values.

Voltage and current controllers tuned through Ziegler Nichols method have been chosen for Voltage Source Inverter. Because voltage and current controllers which are tuned through Ziegler Nichols method are more close to the design specifications listed in section 4.2. It can also be seen in table 3.1 that the bandwidth difference of voltage and current controller got through Chien Hrones Reswick method is very narrow. This narrow difference in bandwidth can affect the performance of a system. It has been suggested in [38] that the bandwidth of current controller should be 10 times greater than the bandwidth of a voltage controller. If this suggestion is set as a standard then the voltage and current controllers tuned through Ziegler Nichols method are the best possible choice even better than robust response time method.

4.4 Synchronization of VSIs

In chapter 3 inverter design has been discussed in detail. All main control blocks are successfully designed and tuned. In this section simulation results will be presented to validate proposed design for different scenarios and load conditions. It has already been discussed that parallel connected inverters with fix droop values are not easy to synchronize when their droop values are different. There is another problem when the line impedance is different for parallel connected inverters then this difference in line impedances may lead the whole system towards instability. The inverter, which is connected in a close vicinity to the load faces less line impedance than inverter which is connected at a comparatively long distance from the load. Therefore the net load

value for each inverter will be different and there will be unequal load sharing. This will lead to an unequal power sharing and then different reference signals for both inverters. In section 2.2.5 it has already been discussed, key parameters have mentioned in that section have a certain kind of influence on the system which were also mentioned in 2.2.5. For the success of design the synchronization process is also needed to examine. The following criteria have been set for this:

1. Both inverters should have same voltage level or voltage difference should not be more than 4%.
2. Both inverters should have the same frequency (for output voltages) or frequency difference should not be more than 1%.
3. Both inverters should not have a phase difference in their two output voltages.

Note: Difference in zero crossing (on the time axis) of two voltages is called phase angle difference [26].

When both inverters have different reference/tracking signals then they will try to approach different steady states which lead them to instability. This problem is encountered using impedance matching technique as discussed in [52] or by using the concept of virtual impedance as suggested in [50]. By keeping the above mentioned problem in mind following Simulink tests are proposed to validate the proposed design:

1. Design validation for a single phase VSI in stand alone mode. This is to analyse its response towards different load conditions and also to analyse its capability to operate with both linear and non-linear loads. Because most of the home appliances act as a non-linear load. If this test is successful then this will give a motivation to put this inverter in parallel with another inverter to form an MG.
2. To identify the problem in parallel connected inverters with fix droop values a Simulink test will be performed. Both parallel connected inverters are first operated with same line impedances and then different line impedances.
3. Then two inverters which are designed through proposed method will be connected in parallel to analyse their behaviour. This is important to check how much improvement is achieved while operating with same and different line impedances.

4.5 Single VSI connected to linear and non-linear load

The first simulation test is performed for a single phase VSI connected to a load in stand alone mode. This simulation test is performed for both linear and nonlinear loads. It can be seen in figure 4.11 and 4.12 that inverter performs very well for both linear and nonlinear loads respectively. It can also be seen in figure 4.1 and 4.2 that even during load variation in point 0.5p.u system retains its stability.

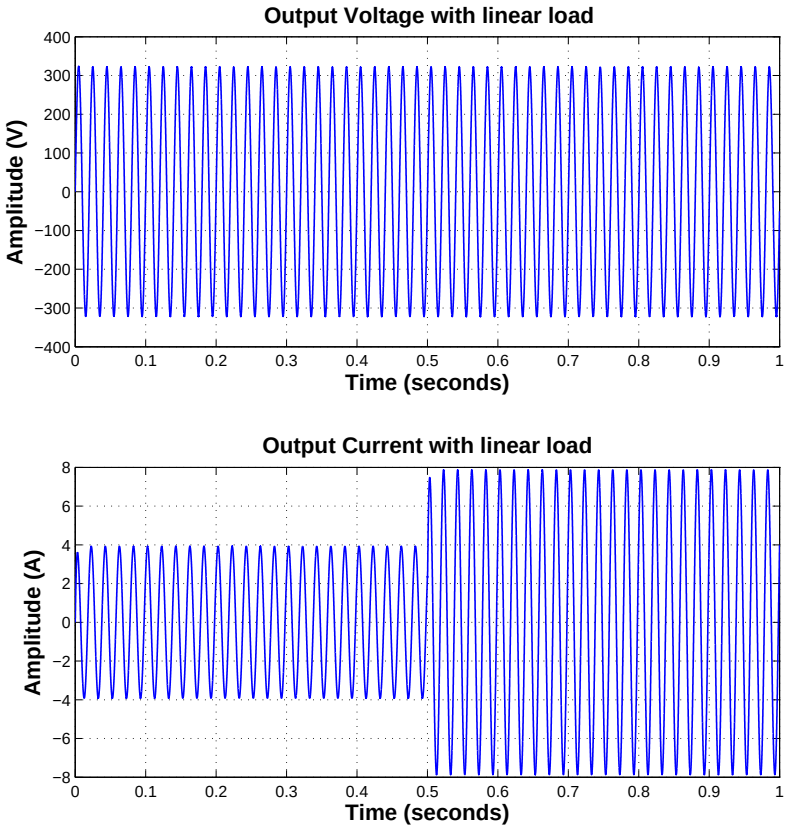

FIGURE 4.11: Output of single VSI with linear load

The output voltage of the system remains almost constant throughout the simulation running time. Simulation results show that there is no overshoot for both voltage and current in linear load case during load transition. The system has very smooth transition response during load variation. In case of non-linear load, the system shows similar results for voltage but for current it can be seen a small overshoot which lasted for half a cycle. This is the only difference in performance of VSI with linear and non-linear load.

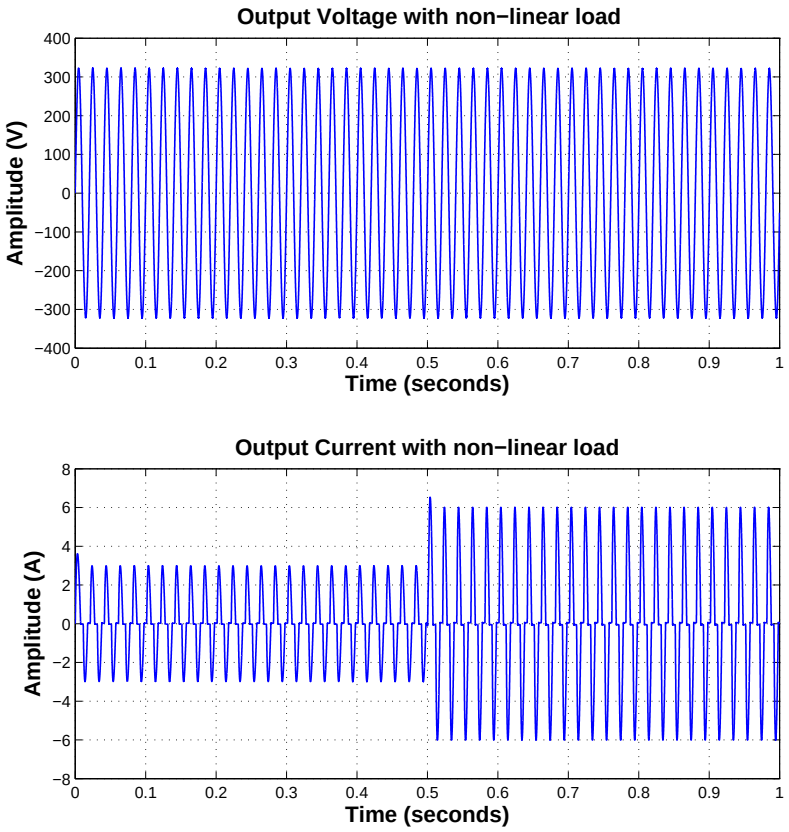

FIGURE 4.12: Output of single VSI with non-linear load

In figure 4.13 and 4.14 active and reactive power for both linear and nonlinear loads has been shown respectively. For linear load variation, output active and reactive power shows very smooth transition without any overshoot.

In figure 4.14 when inverter subjects to a non-linear load there is an overshoot in both active and reactive power. It is a well known fact that the output power is a product of output current and voltage, therefore an overshoot in output current causes this phenomena in active and reactive power.

After these simulation results this is very obvious that the designed inverter has met all expectations that has been assumed at the time of designing. Inverter response towards variations is very encouraging for both voltage and current. Step response of a current controller is shown in figure 4.10, in which overshoot is clearly visible and this has been examined in case of non-linear load. Meanwhile high bandwidth of controller enables it to deal with this situation very quickly and efficiently therefore this overshoot did not last for too long.

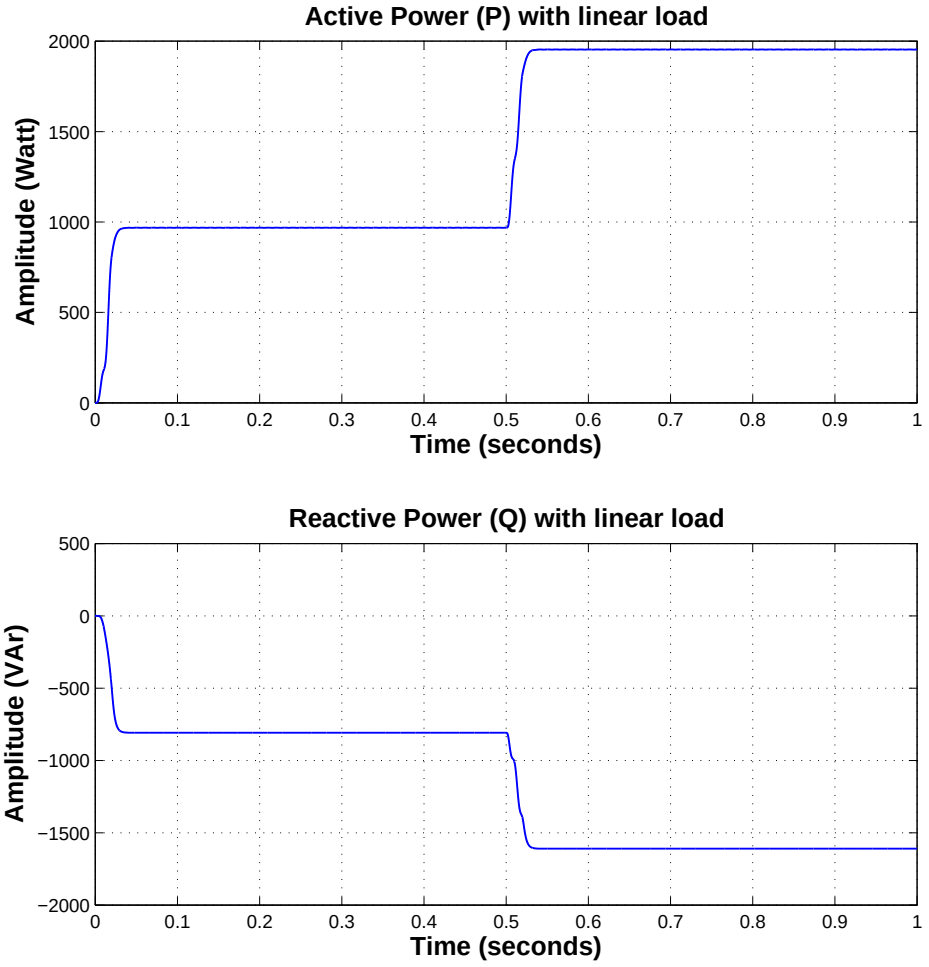

FIGURE 4.13: Output power of single VSI with linear load

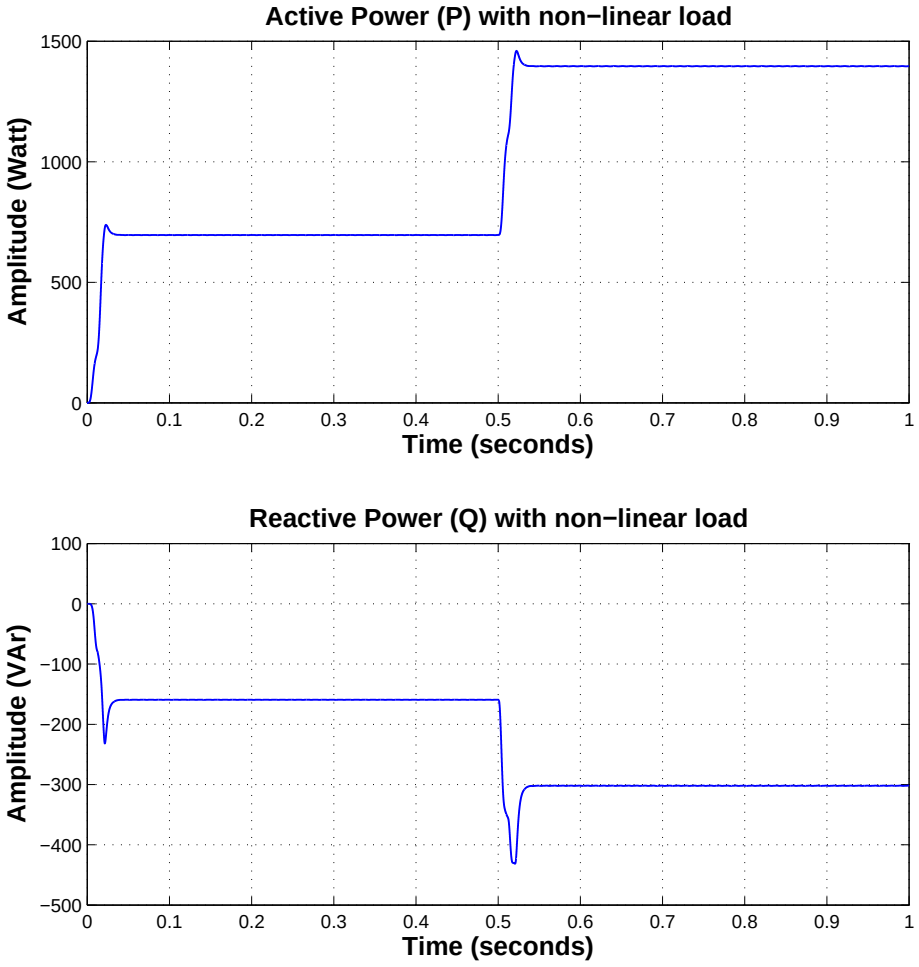

FIGURE 4.14: Output power of single VSI with non-linear load

4.6 Two Parallel connected inverters with fix droop gains

Results for single phase VSI in stand alone mode are satisfactory. In this section simulation test for parallel connected inverters with fix droop gains (which is a conventional technique) will be performed. This will be good to observe and understand a problem, when two inverters have different line impedances which has been addressed by this thesis work. Two scenarios have been built in simulation for parallel connected inverters with fix droop gains which are:

1. Parallel connection with same line impedance.
2. Parallel connection with different line impedance.

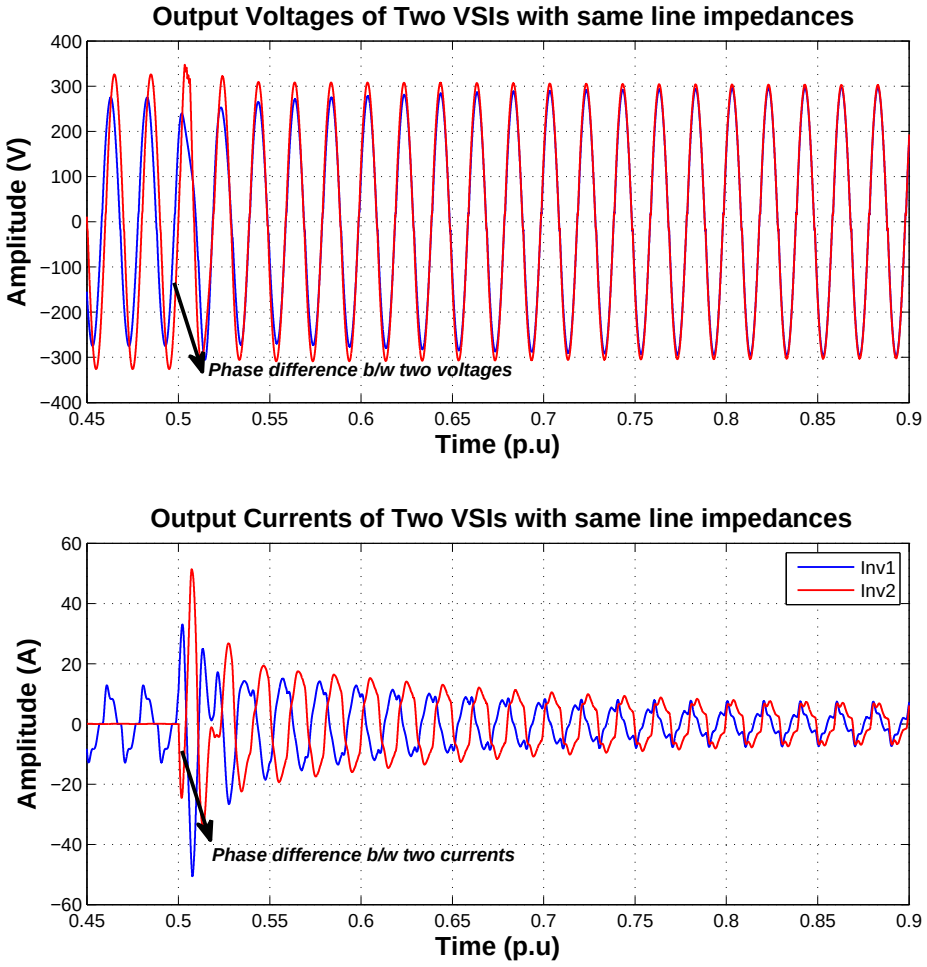

FIGURE 4.15: Output voltage and current of Two parallel connected VSIs with same line impedance

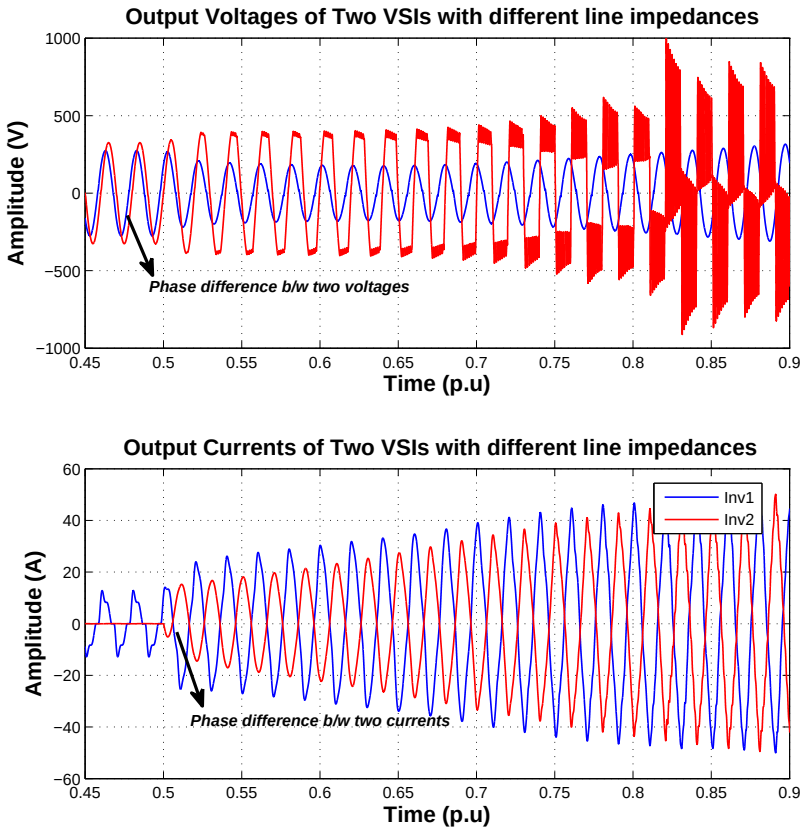

FIGURE 4.16: Output voltage and current of Two parallel connected VSIs with different line impedance

Figure 4.15 shows the performance of two parallel connected inverters having a same line impedance. Initially inverter1 is connected to a non-linear load and inverter2 is not connected to any load. It can be seen in 4.15 that output current of inverter1 is almost around 15A and 0A for inverter2, likewise there is difference in output voltages of two inverters. Sine waves of both voltages crossing zero at different time (p.u), this shows a phase difference between two voltages. A distorted wave form of currents is because of non-linear load as this kind of load induces harmonics in current.

At time 0.5 p.u inverter2 is also connected to the load. It can be seen that at the time of connection both inverters have different output voltages and also have phase difference. After connecting in parallel both inverters tend to synchronize. Synchronization means to achieve same output voltage and same frequency and phase angle for output voltages. It is obvious from figure 4.15 that output voltages of both inverters are overlapping, which shows that both inverters has successfully achieved same frequency or phase and same voltage level. Although at the time of connection a huge spike was visible for current graph, this spike is due to the flow of circulating current between two inverters. Current controller supposes to deal with this issue so, it does and very quickly bring

both currents in the controllable range which is 16A (assumed maximum value current according to an inverter data sheet in lab).

The same simulation test has been performed for different line impedances for each inverter. It is shown in figure 4.16 that after connecting parallel to each other at time 0.5p.u both inverters became unstable. The phase angle difference between two voltages and currents is increased which was gradually reduced to zero in figure 4.15. It can also be seen in figure 4.16 that the voltage and current of both inverters has increased to a very high value. If there is not a safety mechanism like breakers or fuse this can damage the whole system. This instability happens due to different reference/tracking signals for both inverters. Due to their different line impedances both inverters has experienced different net load and produced different amount of output power which is responsible for generating different reference/tracking signals.

4.7 Two Parallel connected inverters with Estimated droop gains

Now simulation results for the proposed estimated droop control scheme will be presented. The same scenario has been built in simulation as for fix droop control gains.

1. Parallel connection with same line impedance.
2. Parallel connection with different line impedance.

First system's performance has been examined with same line impedance for both inverters. It can be seen in figure 4.17 that inverter voltage remains constant throughout the simulation test with a minute difference which is not visible due to overlapping of two signals. Inverter2 is connected to the load at time 0.4p.u, it can be seen that system response is very fast and both inverters are synchronized very quickly. Initially before connecting in parallel, both inverters have a small difference between their output voltages, as soon as they are connected to the same load in parallel they start operating with same voltages. The green signal in a voltage graph of figure 4.17 shows the difference between two voltages because this is not very clear in actual voltage graphs due to overlapping of signals. Both inverters share not only equal voltage level but also current level. Before connecting to the load inverter2 has 0A output current. Then load is decreased at time 0.6p.u and then again increased at time 0.8p.u. During all these variations system response is tremendously fast and stable. A small overshoot can be seen for current as it was expected due to the current controller design. Another most

important parameter after voltage is to maintain system's frequency. In figure 4.17 (the third graph) it can be seen that system maintains its frequency at a standard level which is very encouraging.

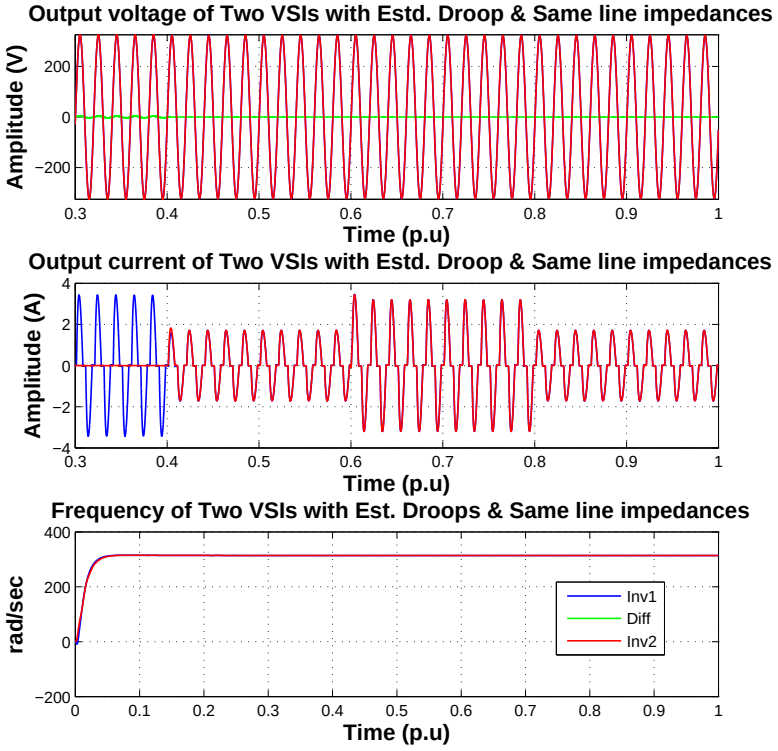

FIGURE 4.17: Output voltage, current and frequency of Two parallel connected VSIs with Est. droop control and same line impedance

Figure 4.18 shows the plot of estimated droop gains. In start when no load is connected to the inverter the droop gains estimator gives random values due to the very minute flow of active and reactive powers. Ideally there should not be a flow of active and reactive power when the switches are open but in Matlab/Simulink switches (even ideal switches) has this problem. Therefore, it shows some spikes before closing the switch, these spiked are suppressed to have prominent visibility of droop gain lines. It can be seen that inverter1 is connected to the load first in simulation, the blue line shows the value of droop gains for inverter1. Inverter2 is connected to the load at time 0.4p.u before this droop gain of inverter2 are zero because inverter2 was not connected to the load and it is in free running mode. After connecting in parallel, both inverters automatically achieve same droop gain values for frequency droop gains and almost same with a slight difference for voltage droop gains. One thing is very important to note is that no predefined droop gains are being used as it happens in conventional fix droop control scheme. This designed system is estimating and updating these droop gain values online. It is also very obvious from figure 4.18 that both inverters keep

same droop gain values even during different variations in load. These same droop gain values for both inverters ensure almost equal power sharing and same reference/tracking signals for both inverters. When reference/tracking signals are same then both inverters will tend to achieve a same steady state. Simulation results for equal power sharing has been shown in figure 4.19, where a small difference in reactive power sharing can be seen which is not affecting the performance of the proposed system.

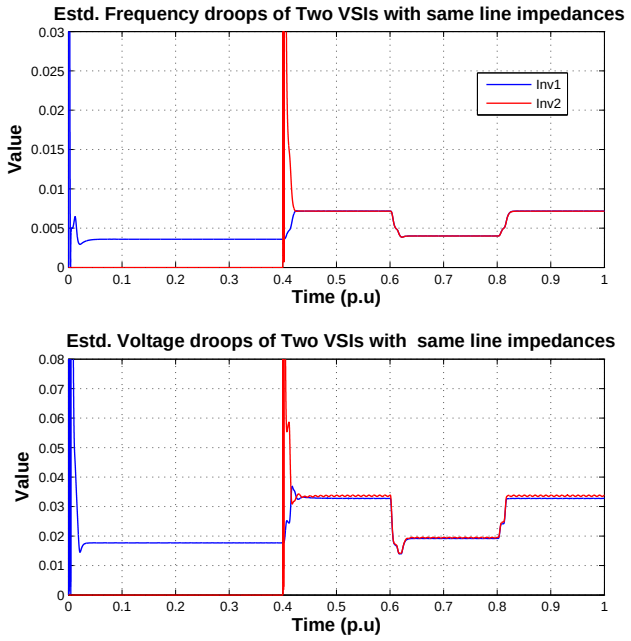

FIGURE 4.18: Frequency and Voltage droop gains of Two parallel connected VSIs with Est. droop control and same line impedance

Now the simulation results for parallel connected inverters with different line impedance will be shown. This is the most important test which will give surety of success for proposed design methodology. It has already been shown in figure 4.16 that the conventional fix droop gain method has failed to tackle this problem (in different line impedance case) which makes a system unstable due to the flow of huge voltages and currents into the system which are the result of lack of synchronization.

Simulation results in figure 4.20 shows that output voltages of both inverters have very small voltage difference and remains almost at the same level during different variations in load and system. In case of output current results are different because of unequal line impedance for each inverter. It is a well know fact that current is inversely proportional to the resistance/impedance of a system. Let's say line impedance of inverter1 is Z_1 and line impedance for inverter2 is Z_2 such that $Z_1 \neq Z_2$. When the line impedance for each inverter is different and both inverters are connected to the load then both inverters will experience different net load.

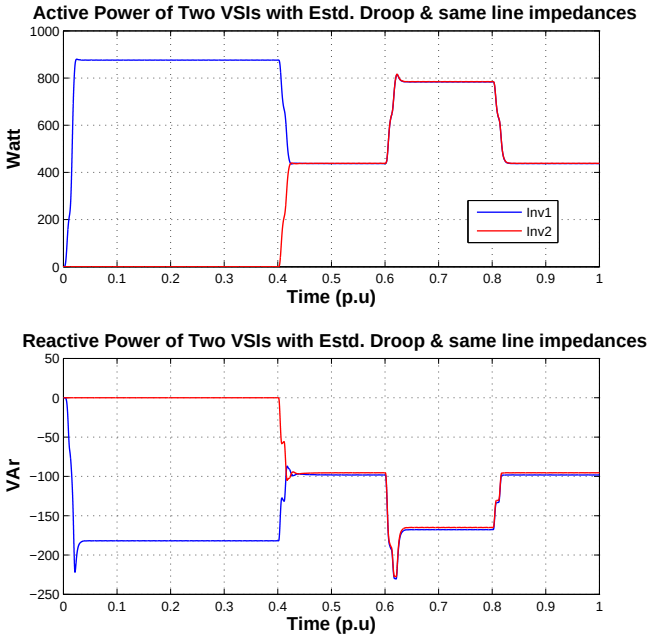

FIGURE 4.19: Output active and reactive of Two parallel connected VSIs with Est. droop control and same line impedance

$$Loadforinverter1 = Load + Z_1 \tag{4.2}$$

$$Loadforinverter2 = Load + Z_2 \tag{4.3}$$

Therefore both inverters are supposed to inject a different amount of current into the load. Inverter1 has experienced more load so it is injecting less current than inverter2. This is shown in figure 4.20 that both inverters injecting different currents into the load. This is also a noticeable fact though both inverter producing different output currents and there is a phase angle difference between two currents but still the operation of is synchronized and stable. In figure 4.16 it can be seen that phase shift between two output currents in the traditional droop control system is almost 180^o. In figure 4.20 this phase shift is almost 90^o. This gives a conclusion that when there is a 180^o phase difference between two currents then this will disturb phase difference between two voltages. It will also tend to bring the small phase difference between voltages to 180^o which eventually affects the synchronization process for two inverters and make the system unstable due to high voltage and current flow into the system. In the proposed method of estimated droop control, the system keeps almost 90^o phase difference and did not let it exceed. Therefore both voltages of inverter1 and inverter2 are unaffected. This is very encouraging that system has kept its synchronization and stability even with different line impedance. The second most important factor is the frequency of the

entire system, which is stable at its nominal value during the simulation running time frequency graph is shown in figure 4.20 (the third plot). It is obvious from figure 4.20 that system not only keep its voltage at constant level but also the frequency.

It has already been discussed that why the system gets unstable for different line impedances with fix droop gains. System with estimated droop gains for different line impedances remain stable because each inverter in a system is responsible to adjust its droop gains according to its total output impedance so that their reference/tracking signals remain unaffected.

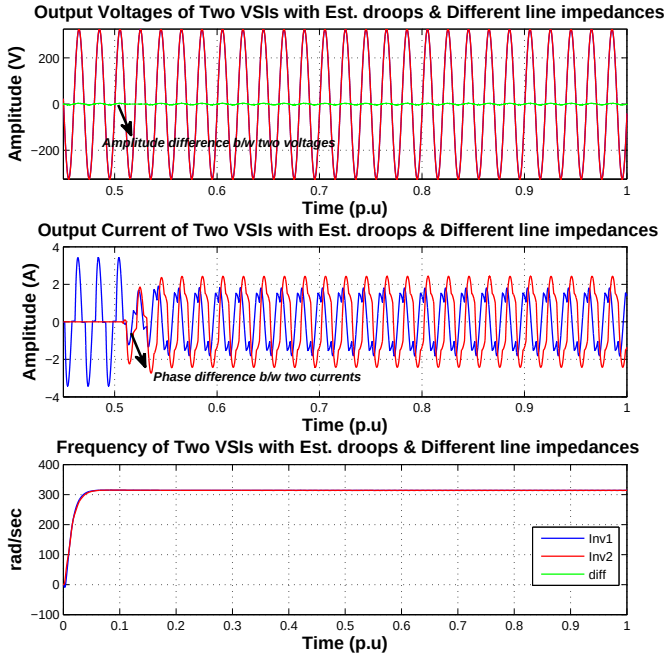

FIGURE 4.20: Output voltage, current and frequency of Two parallel connected VSIs with Est. droop control and different line impedance

In figure 4.21 it can be seen that both inverters have adjusted their droop gains according to their output impedance and output power. When load varies at time 1p.u and 1.5p.u respectively both inverters adjust their droop values without losing their synchronization and stability.

Output active and reactive power of both parallel connected inverters is shown in figure 4.22. It can be seen that both inverters are delivering different amount of active and reactive power to the load. This is very difficult to synchronize two or more parallel connected inverters with different droop gains and unequal power sharing. Simulation results show that an inverter with the proposed design scheme is well capable to deal with such kind of problems. This proposed scheme has increased the stability of the system.

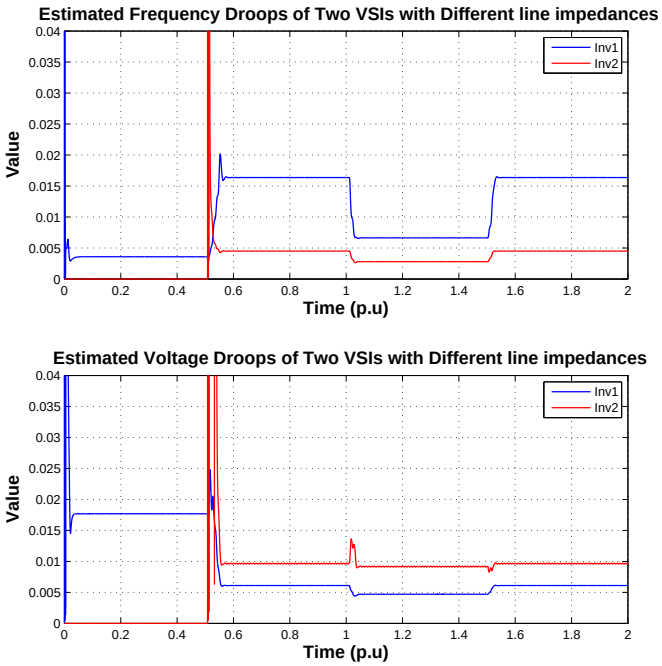

FIGURE 4.21: Frequency and Voltage droop gains of Two parallel connected VSIs with Est. droop control and different line impedance

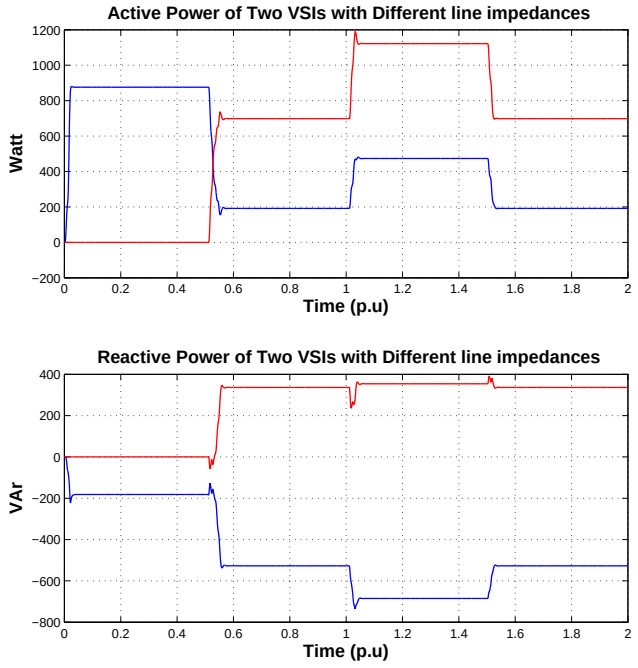

FIGURE 4.22: Output active and reactive of Two parallel connected VSIs with Est. droop control and different line impedance

Chapter 5

Conclusion

The entire electric supply system is going through very important changes. Demand for energy is increasing day by day to fulfil this demand scientist have to look for all available sources. Because depending only on fossil fuel resources may lead to a big crisis in future as fossil fuel reserves are finite. Distributed energy sources including RES entering into the present day energy market with a promise of future growth. These distributed energy resources are small in size as compared to the existing power supply system but they are large in numbers. This fundamental change in structure and design asks for a completely new mechanism for their operation in order to harvest and integrate these energy resources. These energy resources are mostly dependent on external factors like wind speed, intensity of sunlight etc. Researchers are motivated to work on these problems to meet set goals in the future. This thesis work is also an effort to meet these goals.

This thesis work is conducted to improve the stability and reliability of low and medium voltage Mirogrids consisting of more than one RES. Grid forming inverters are used as an interface between main utility grid and these RES. These inverters are used to extract power from these RES units and then process it according to the requirements of main utility grid and local load.

Different techniques for inverter design has been studied which are in use nowadays. A brief review of the existing power system structure is included for understanding how the conventional power system is working. Then Microgrid system is explained in detail including its structure and all fundamental parameters which can affect its performance. To improve the reliability of a system a non-communication based technique is preferred namely "Estimated Droop Control". The proposed design methodology has been explained step by step for all important blocks given by

1. PWM Modelling
2. Plant Modelling
3. Power Calculation Block
4. Droop Estimation and Reference signal Generation
5. Inner Control Blocks

The droop gains for each inverter are estimated online and then adapted by each inverter. The amplitude estimation of the inverter output voltage is done by using a generalized integrator, its gains are provided by Kalman estimator. The phase and frequency of the inverter output voltage are estimated by a PLL technique with Kalman estimator.

Then the results are shown and compared with the conventional droop control scheme. This comparison shows that the estimated droop control not only improves the stability of the system but also improves the reliability. The reliability is of more concern about how much an inverter is independent in its operations. In the conventional droop control scheme droop gains of an inverter are used as (virtual) means of communication with one another in same microgrid. In the Estimated droop control scheme these droop gains are estimated online and no predefined values are used. This method increases the reliability of a system by freeing each inverter in a system from this only virtual communication link. Stability is also improved by this proposed technique as it is shown by simulation results especially in case of different line impedance.

5.1 Future Work

This proposed scheme is only tested for single phase inverters. For future work, this technique can be modified for three phase system. A thorough study can be conducted for total harmonic distortion effect due to both linear and non-linear loads. More sophisticated and modern control techniques can be used to tune voltage and current controllers like robust control, model predictive control, LQG which may improve the performance of voltage and current controller.

Bibliography

[1] R. Majumder, *Modeling, stability analysis and control of microgrid.* Queensland University of Technology, 2010.

[2] Y. A.-R. I. Mohamed, *New control algorithms for the distributed generation interface in grid-connected and micro-grid systems.* PhD thesis, University of Waterloo, 2008.

[3] T. Ackermann *et al.*, *Wind power in power systems*, vol. 140. Wiley Online Library, 2005.

[4] B. C. Ummels, M. Gibescu, E. Pelgrum, W. L. Kling, and A. J. Brand, "Impacts of wind power on thermal generation unit commitment and dispatch," *Energy Conversion, IEEE Transactions on*, vol. 22, no. 1, pp. 44–51, 2007.

[5] E. Muljadi, C. Butterfield, B. Parsons, and A. Ellis, "Effect of variable speed wind turbine generator on stability of a weak grid," *Energy Conversion, IEEE Transactions on*, vol. 22, no. 1, pp. 29–36, 2007.

[6] T. Petru and T. Thiringer, "Modeling of wind turbines for power system studies," *Power Systems, IEEE Transactions on*, vol. 17, no. 4, pp. 1132–1139, 2002.

[7] G. A. Raducu, "Control of grid side inverter in a b2b configuration for wt applications," *PED10-1015b, Aalborg University*, 2008.

[8] D. Hopwood, "Abu dhabi's masdar plan takes shape," *Renewable Energy Focus*, vol. 11, no. 1, pp. 18–23, 2010.

[9] S. Nader, "Paths to a low-carbon economythe masdar example," *Energy Procedia*, vol. 1, no. 1, pp. 3951–3958, 2009.

[10] L. B. Microgrids, "Ieee power engineering society winter meeting," *New York*, pp. 146–149, 2001.

[11] N. Pogaku, M. Prodanovic, and T. C. Green, "Modeling, analysis and testing of autonomous operation of an inverter-based microgrid," *Power Electronics, IEEE Transactions on*, vol. 22, no. 2, pp. 613–625, 2007.

[12] M. Suter, *Active filter for a microturbine*. IET, 2001.

[13] R. Billinton, M. Fotuhi-Firuzabad, and L. Bertling, "Bibliography on the application of probability methods in power system reliability evaluation 1996-1999," *Power Systems, IEEE Transactions on*, vol. 16, no. 4, pp. 595–602, 2001.

[14] M. Etezadi-Amoli and K. Choma, "Electrical performance characteristics of a new micro-turbine generator," in *Power Engineering Society Winter Meeting, 2001. IEEE*, vol. 2, pp. 736–740, IEEE, 2001.

[15] S. Yang, C. Zhang, X. Zhang, R. Cao, and W. Shen, "Study on the control strategy for parallel operation of inverters based on adaptive droop method," in *Industrial Electronics and Applications, 2006 1ST IEEE Conference on*, pp. 1–5, IEEE, 2006.

[16] J. Machowski, J. Bialek, and J. Bumby, *Power system dynamics: stability and control*. Wiley, 2011.

[17] P. Kundur, *Power system stability and control*, vol. 12. Tata McGraw-Hill Education, 2001.

[18] O. Osika, *Stability of micro-grids and inverter-dominated grids with high share of decentralised sources*. Kassel University Press, 2005.

[19] V. Engineering Photos and Articles, "Chapter 2 ac generators." http://emadrlc.blogspot.de/2013/01/chapter-2-ac-generators.html, 2013.

[20] Y. X. Wenping Cao and Z. Tan, "Wind turbine generator technologies." http://www.intechopen.com/books/advances-in-wind-power/wind-turbine-generator-technologies, 2012.

[21] N. Mohan and T. M. Undeland, *Power electronics: converters, applications, and design*. John Wiley & Sons, 2007.

[22] M. H. Rashid, *Power electronics handbook*. Academic Pr, 2001.

[23] K. De Brabandere, "Voltage and frequency droop control in low voltage grids by distributed generators with inverter front-end (spannings-en frequentieregeling in laagspanningsnetten door gedistribueerde opwekkers met vermogenelektronische netkoppeling)," *status: published*, 2006.

[24] D. P. Ariyasinghe and D. M. Vilathgamuwa, "Stability analysis of microgrids with constant power loads," in *Sustainable Energy Technologies, 2008. ICSET 2008. IEEE International Conference on*, pp. 279–284, IEEE, 2008.

[25] N. L. Soultanis, S. A. Papathanasiou, and N. D. Hatziargyriou, "A stability algorithm for the dynamic analysis of inverter dominated unbalanced lv microgrids," *Power Systems, IEEE Transactions on*, vol. 22, no. 1, pp. 294–304, 2007.

[26] A. Mazloomzadeh, V. Salehi, and O. Mohammed, "Soft synchronization of dispersed generators to micro grids for smart grid applications," in *Innovative Smart Grid Technologies (ISGT), 2012 IEEE PES*, pp. 1–7, IEEE, 2012.

[27] H. Van Der Broeck and U. Boeke, "A simple method for parallel operation of inverters," in *Telecommunications Energy Conference, 1998. INTELEC. Twentieth International*, pp. 143–150, IEEE, 1998.

[28] J.-F. Chen and C.-L. Chu, "Combination voltage-controlled and current-controlled pwm inverters for ups parallel operation," *Power Electronics, IEEE Transactions on*, vol. 10, no. 5, pp. 547–558, 1995.

[29] S. Shah, *Design & Implementation of Parallel Operation of Inverters with Instantaneous Current Sharing Scheme Using Multiloop Control Strategy on FPGA Platform*. PhD thesis, Indian Institute of Technology, 2008.

[30] T. Kawabata and S. Higashino, "Parallel operation of voltage source inverters," *Industry Applications, IEEE Transactions on*, vol. 24, no. 2, pp. 281–287, 1988.

[31] B. Burger and A. Engler, "Fast signal conditioning in single phase systems," in *9th European Conference on Power Electronics and Applications*, vol. 27, 2001.

[32] A. Haddadi, A. Shojaei, and B. Boulet, "Enabling high droop gain for improvement of reactive power sharing accuracy in an electronically-interfaced autonomous microgrid," in *Energy Conversion Congress and Exposition (ECCE), 2011 IEEE*, pp. 673–679, IEEE, 2011.

[33] C. Rowe, T. Summers, and R. Betz, "Arctan power frequency droop for power electronics dominated microgrids," in *Universities Power Engineering Conference (AUPEC), 2010 20th Australasian*, pp. 1–6, IEEE, 2010.

[34] J. C. Vasquez, J. M. Guerrero, A. Luna, P. Rodríguez, and R. Teodorescu, "Adaptive droop control applied to voltage-source inverters operating in grid-connected and islanded modes," *Industrial Electronics, IEEE Transactions on*, vol. 56, no. 10, pp. 4088–4096, 2009.

[35] M. Kohansal, J. S. Moghani, M. Rahmatian, and G. B. Gharehpetian, "An approach to decrease transient circulating current of vsis in islanded microgrid," *International Conference on Renewable Energies and Power Quality*, 2012.

[36] J. Matas, M. Castilla, L. G. de Vicuña, J. Miret, and J. C. Vasquez, "Virtual impedance loop for droop-controlled single-phase parallel inverters using a second-order general-integrator scheme," *Power Electronics, IEEE Transactions on*, vol. 25, no. 12, pp. 2993–3002, 2010.

[37] N. Mohan and T. M. Undeland, *Power electronics: converters, applications, and design*. Wiley. com, 2007.

[38] G. M. Azevedo, M. C. Cavalcanti, F. A. Neves, P. Rodriguez, and J. Rocabert, "Performance improvement of the droop control for single-phase inverters," in *Industrial Electronics (ISIE), 2011 IEEE International Symposium on*, pp. 1465–1470, IEEE, 2011.

[39] J. C. Vasquez, J. M. Guerrero, M. Savaghebi, and R. Teodorescu, "Modeling, analysis, and design of stationary reference frame droop controlled parallel three-phase voltage source inverters," in *Power Electronics and ECCE Asia (ICPE & ECCE), 2011 IEEE 8th International Conference on*, pp. 272–279, IEEE, 2011.

[40] B. Crowhurst, E. El-Saadany, L. El Chaar, and L. Lamont, "Single-phase grid-tie inverter control using dq transform for active and reactive load power compensation," in *Power and Energy (PECon), 2010 IEEE International Conference on*, pp. 489–494, IEEE, 2010.

[41] B. Sohlberg, *Applied Model Based Control*. Karlstad University Press, 2008.

[42] L. Kleeman, "Understanding and applying kalman filtering." http://www.cs.cmu.edu/~motionplanning/papers/sbp_papers/integrated3/kleeman_kalman_basics.pdf, 2013.

[43] L. G. B. Rolim, D. R. da Costa, and M. Aredes, "Analysis and software implementation of a robust synchronizing pll circuit based on the pq theory," *Industrial Electronics, IEEE Transactions on*, vol. 53, no. 6, pp. 1919–1926, 2006.

[44] J. Costa, D.R., L. G. B. Rolim, and M. Aredes, "Analysis and software implementation of a robust synchronizing circuit pll circuit," in *Industrial Electronics, 2003. ISIE '03. 2003 IEEE International Symposium on*, vol. 1, pp. 292–297 vol. 1, 2003.

[45] A. Julean, "Active damping of lcl filter resonance in grid connected applications," *Aalborg Universitet, Dinamarca, Dissertação de mestrado*, 2009.

[46] J. Lettl, J. Bauer, and L. Linhart, "Comparison of different filter types for grid connected inverter," *PIERS Proceedings*, 2011.

[47] A. Dash, B. C. Babu, K. Mohanty, and R. Dubey, "Analysis of pi and pr controllers for distributed power generation system under unbalanced grid faults," in *Power and Energy Systems (ICPS), 2011 International Conference on*, pp. 1–6, IEEE, 2011.

[48] N. Pogaku, M. Prodanovic, and T. C. Green, "Modeling, analysis and testing of autonomous operation of an inverter-based microgrid," *Power Electronics, IEEE Transactions on*, vol. 22, no. 2, pp. 613–625, 2007.

[49] J. Matas, M. Castilla, L. G. de Vicuña, J. Miret, and J. C. Vasquez, "Virtual impedance loop for droop-controlled single-phase parallel inverters using a second-order general-integrator scheme," *Power Electronics, IEEE Transactions on*, vol. 25, no. 12, pp. 2993–3002, 2010.

[50] R. C. Dorf, *Modern control systems*. Addison-Wesley Longman Publishing Co., Inc., 1991.

[51] D. Xue, D. P. Atherton, and Y. Chen, *Linear feedback control: analysis and design with MATLAB*. Siam, 2007.

[52] H. Gu, X. Guo, and W. Wu, "Accurate power sharing control for inverter-dominated autonomous microgrid," in *Power Electronics and Motion Control Conference (IPEMC), 2012 7th International*, vol. 1, pp. 368–372, IEEE, 2012.

Appendix A

Kalman Filter Design

Kalman Filter is an extension of an observer. This is used for the estimation of process states by an assumption in disturbances acting on states of a process and measured outputs. For designing a Kalman filter let's suppose a following model.

$$\hat{x} = Ax + Bu + Gw \tag{A.1}$$

$$y = Cx + Du + v \tag{A.2}$$

Where $B = 0$ and $D = 0$ because there is no measured input $u(t)$. Process input and output white noises are w and v. Covariances of two noises are $Q = E[ww^T]$ and $R = E[vv^T]$

$$e = x - \hat{x} \tag{A.3}$$

$$P = E[ee^T] = E[(x - \hat{x})(x - \hat{x})^T] \tag{A.4}$$

Where P is error covariance matrix

New estimation with measured data can be written as

$$\hat{x} = \overline{x} + K(y - C\overline{x}) \tag{A.5}$$

Where $\overline{x}$ is prior estimate of $\hat{x}$

Now substitute Eq. (A.2) into Eq.(A.5)

$$\hat{x} = \overline{x} + K(Cx + v - C\overline{x}) \tag{A.6}$$

Now substitute Eq. (A.6) into Eq.(A.4)

$$P = E[(x - \overline{x} - K(Cx + v - C\overline{x}))(x - \overline{x} - K(Cx + v - C\overline{x}))^T] \tag{A.7}$$

$$P = E[[(x - \overline{x})(I - KC) - Kv)][(x - \overline{x})(I - KC) - Kv)]^T] \tag{A.8}$$

$$P = (I - KC)E[(x - \overline{x})(x - \overline{x})^T](I - KC)^T + KE[vv^T]K^T \tag{A.9}$$

Where $x - \overline{x}$ is prior estimation error. so Eq. (A.9) will be rewritten as

$$P = (I - KC)\overline{P}(I - KC)^T + KRK^T \tag{A.10}$$

where $\overline{P}$ is prior estimate of P

Eq (A.10) will give

$$P = \overline{P} - \overline{P}KC - \overline{P}(KC)^T + K(CPC^T + R)K^T \tag{A.11}$$

State prediction Covariance is

$$P = A\overline{P}A^T + Q \tag{A.12}$$

Minimize problem gives following solution

$$K = APC^T[H\overline{P}H^T + R]^{-1} \tag{A.13}$$

Where K is a Kalman gain.

Now substitute Eq.(A.13) into Eq.(A.11)

$$P = \overline{P} - \overline{P}C^T(H\overline{P}H^T + R)^{-1}H\overline{P} \tag{A.14}$$

Now put this value in Eq. (A.12)

$$P = A(\overline{P} - \overline{P}C^T(H\overline{P}H^T + R)^{-1}H\overline{P})A^T + Q \tag{A.15}$$

Eq. (A.13) and (A.15) are the part of recursive functions. An initial guess is needed for $P(0)$ when an observer starts to estimate the state vector. After few iterations P converges to a constant value so that Kalman gain matrix K also achieves a constant value. Number of iterations depends on how much smart initial guess has been used and for a successful convergence, pair of A, C should be completely observable. In Matlab **kalman.m** function can be used to find a Kalman gain matrix as this command is used in following code:

```
w = 314;
q = 0.001;
A = [ 0 -w; w 0];
b = [ 1 ; 0];
g = [ 0 ; 1];
B = [b g];
C = [1 0];
D = 0;
OSC = ss(A,B,C,D)
Q=2/q^2*eye(2)
R=1
[sys,K] = kalman(OSC,Q,R)
```

Appendix B

Tuning methods and System Response

B.1 Controller tuning with Chien-Hrones-Reswick Method

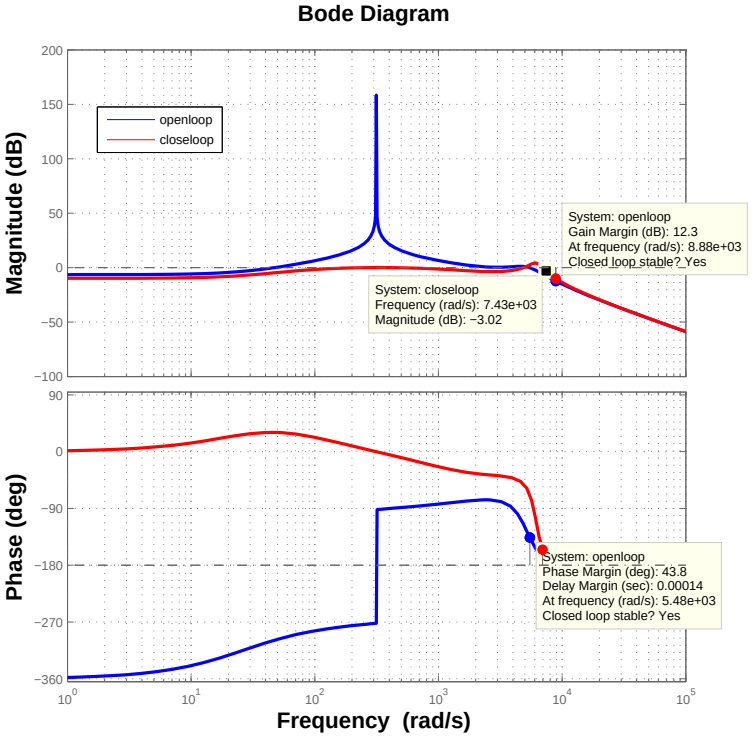

FIGURE B.1: Bode plot of transfer function $G_v(s)$ with compensation through Chien-Hrones-Reswick method

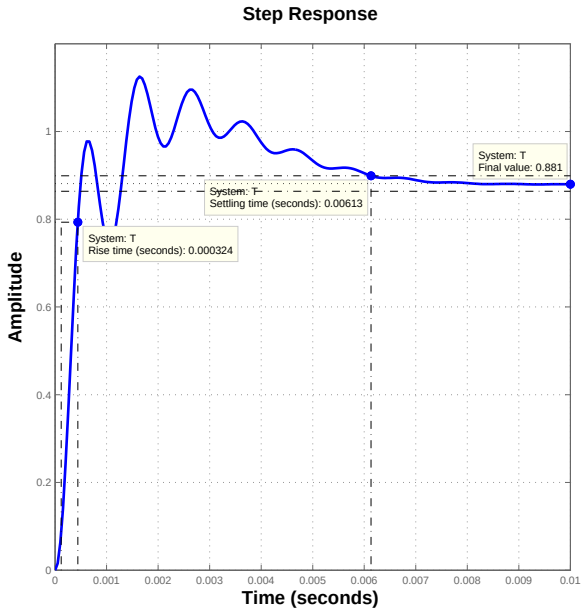

FIGURE B.2: Step response of transfer function $G_v(s)$ with compensation through Chien-Hrones-Reswick method

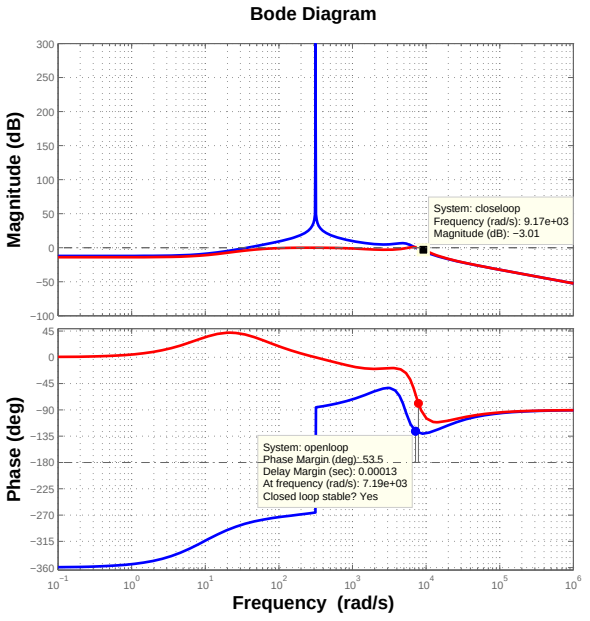

FIGURE B.3: Bode plot of transfer function $G_i(s)$ with compensation through Chien-Hrones-Reswick method

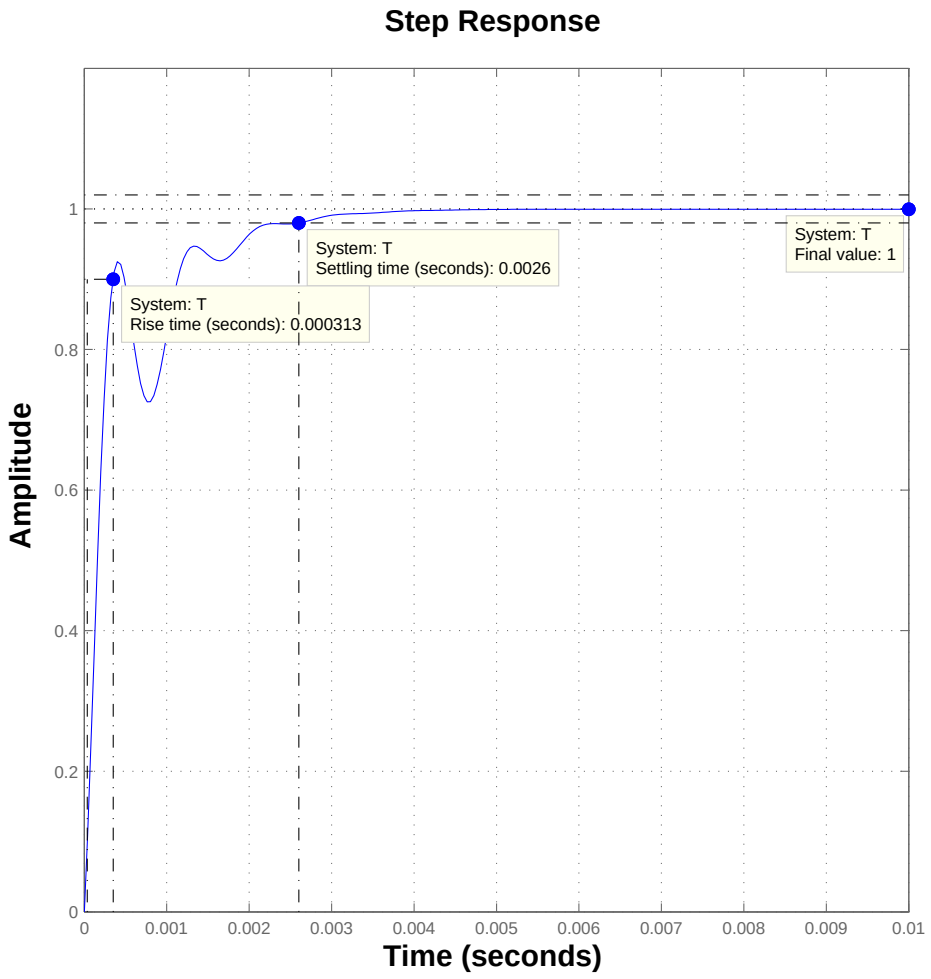

FIGURE B.4: Step response of transfer function $G_i(s)$ with compensation through Chien-Hrones-Reswick method

B.2 Controller tuning with Robust response time method

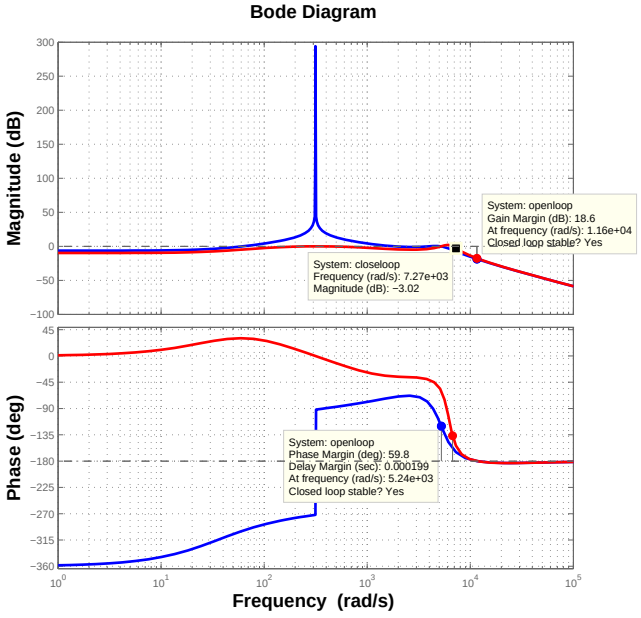

FIGURE B.5: Bode plot of transfer function $G_v(s)$ with compensation through Robust response time method

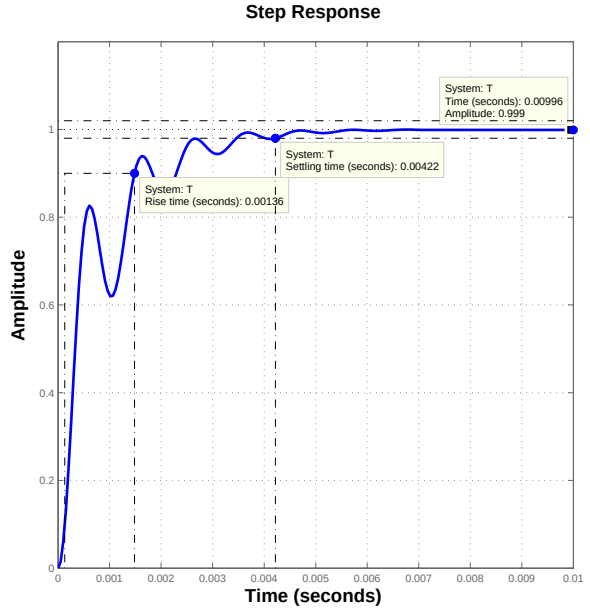

FIGURE B.6: Step response of transfer function $G_v(s)$ with compensation through Robust response time method

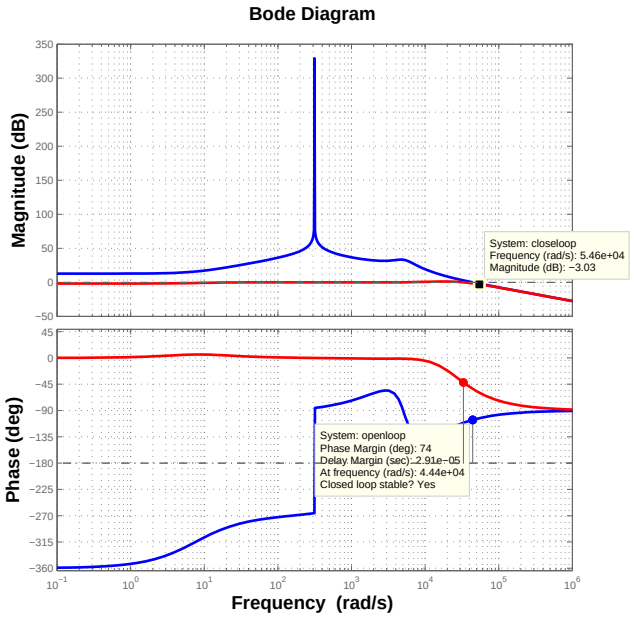

FIGURE B.7: Bode plot of transfer function $G_i(s)$ with compensation through Robust response time method

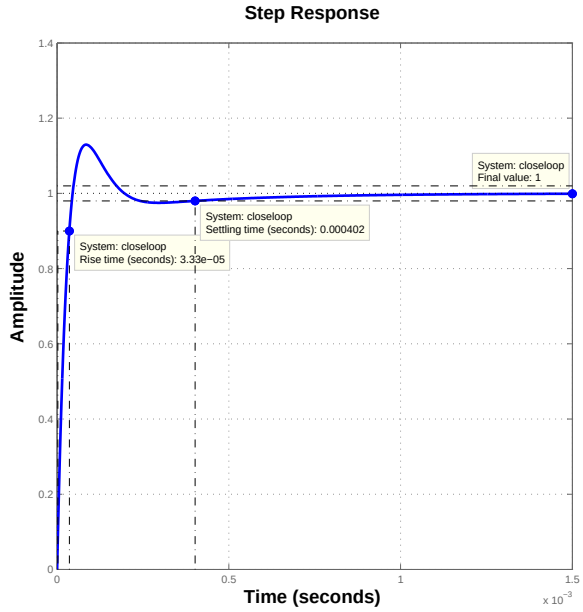

FIGURE B.8: Step response of transfer function $G_i(s)$ with compensation through Robust response time method

Appendix C

Matlab Simulink Model

C.1 Simulink model of a single VSI

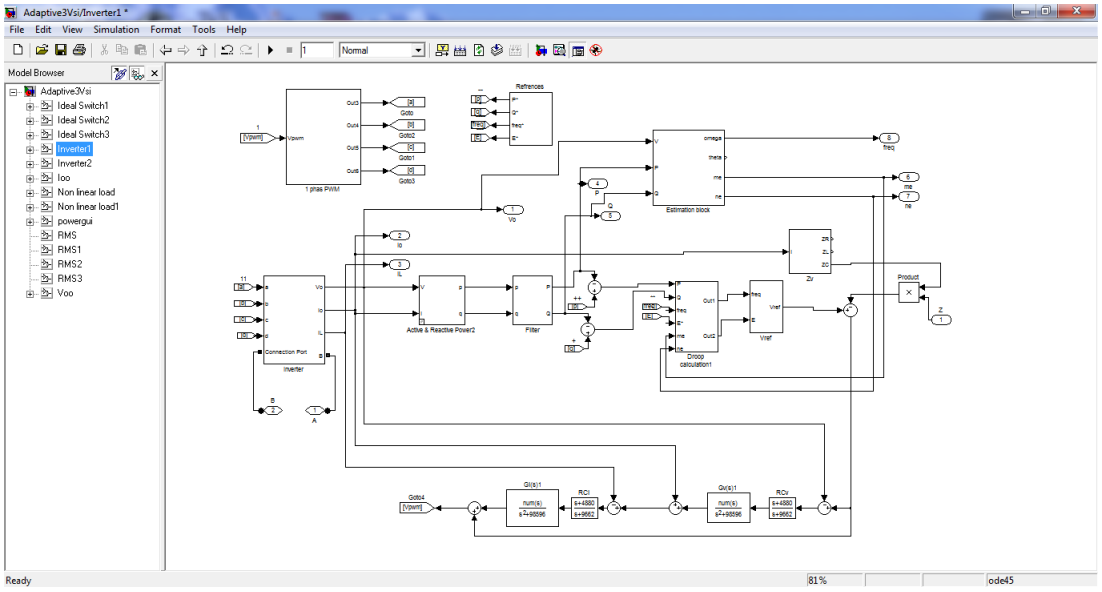

FIGURE C.1: Simulink model of single VSI

C.2 Simulink model of two parallel connected VSIs

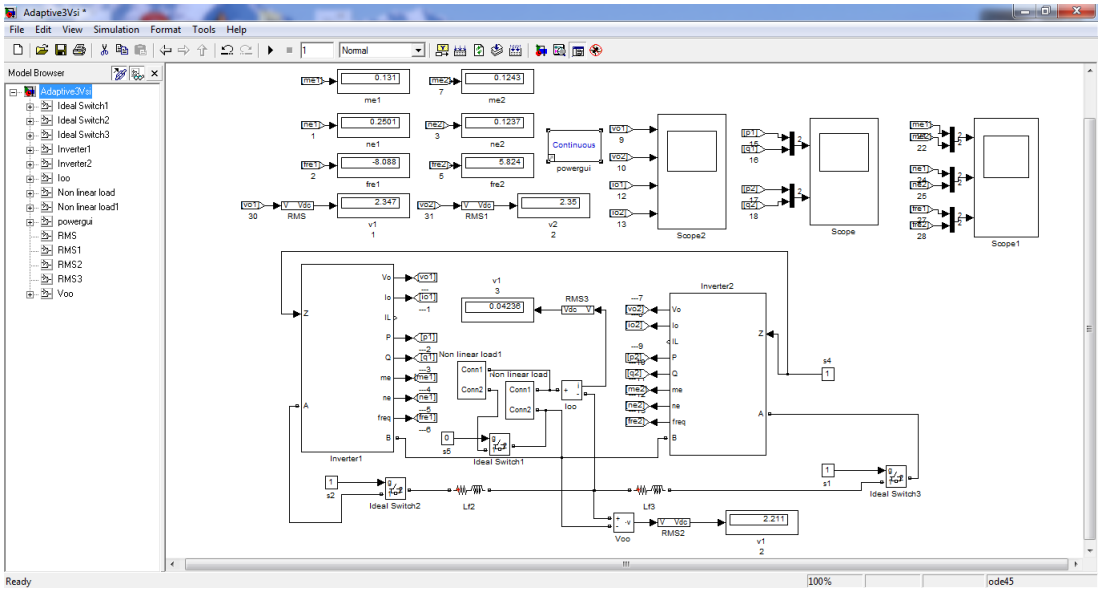

FIGURE C.2: Simulink model of two parallel connected VSIs